Parameterizing complex root water uptake models – the arrangement of root hydraulic properties within the root architecture affects dynamics and efficiency of root water uptake

M. Bechmann[1], C. Schneider[2], A. Carminati[3], D. Vetterlein[4], S. Attinger[2], A. Hildebrandt[1,5]

[1]{Friedrich Schiller University, Jena, Germany, Institute of Geosciences, Burgweg 11, 07749 Jena, Germany}

[2]{Helmholtz Centre for Environmental Research, Leipzig, Germany, Department Computational Hydrosystems, Permoser Straße 15, 04318 Leipzig, Germany}

[3]{Georg-August-University, Göttingen, Germany, Faculty of Agricultural Sciences, Department of Crop Sciences, Büsgenweg 2, 37077 Göttingen, Germany}

[4]{Helmholtz Centre for Environmental Research, Halle, Germany, Department of Soil Physics, Theodor-Lieser-Strasse 4, 06120 Halle/Saale, Germany}

[5]{Max-Planck-Institute for Biogeochemistry, Jena, Germany, Hans-Knöll-Str. 10, 07745 Jena, Germany}

Correspondence to: M. Bechmann (Bechmann.marcel@uni-jena.de)

Abstract

Detailed three-dimensional models of root water uptake have become increasingly popular for investigating the process of root water uptake. However they suffer from a lack of information on important parameters, especially distribution of root hydraulic properties. In this paper we explore the role that arrangement of root hydraulic properties and root system topology play for modelled uptake dynamics. We apply microscopic models of single root structures to investigate the mechanisms shaping uptake dynamics and demonstrate the effects in a complex three dimensional root water uptake model. We introduce two indices to measure the efficiency of root water uptake in terms of "benefits" and "costs", called "water yield" and "effort" respectively. We show that an appropriate arrangement of root hydraulic properties can considerably increase modelled efficiency of root water uptake in single roots, branched roots and entire root systems.

Over the entire transpiration period, the average uptake depth of entire root systems was not much influenced by their hydraulic parameterization. However, other factors such as evolution of collar potential, which is related to the effective resistance to root water uptake of the entire soil-plant-continuum, root bleeding, redistribution patterns and momentary uptake depth were strongly affected by the parameterization. Root systems are more efficient when they are assembled of different root types, allowing for separation of root function in uptake (short young) roots and transport (longer mature) roots. Results become similar, as soon as this composition is accounted for to some degree (between 40 and 80 % of young uptake roots). Effort was decreased up to 40 % and water yield was increased up to 25 % in these composed root systems, compared to homogenous root systems. Also, one parameterization (homogenous young root system) was characterized by excessive bleeding (hydraulic lift), which was accompanied by the lowest efficiency. We conclude that heterogeneity of root hydraulic properties is a critical component of complex three dimensional uptake models. Efficiency measures together with information on critical xylem potentials may be useful in identifying efficient root property distributions.

1 Introduction

Soil-plant interactions are important factors in hydrological and ecological processes. By using soil water for transpiration, plants are the essential link in the mass and energy transfer

at the soil-vegetation-atmosphere-interface (Shukla and Mintz, 1982). Much of this interaction hinges upon the ability of plants to gain flexible access to soil water (Churkina and Running, 1998;Kleidon and Heimann, 2000;Feddes et al., 2001;Hildebrandt and Eltahir, 2007;Collins and Bras, 2007;Katul et al., 2012). Inversely, changes in soil water content reflect on energy partitioning and carbon fluxes at the soil surface (Kleidon and Heimann, 1998;El Maayar et al., 2009;Seneviratne et al., 2010). Furthermore, access to soil water is an important prerequisite for biomass production, including crops (Blum, 1996;Huszár et al., 1998;Cai et al., 2009).

The ubiquitous influence of root water uptake on soil as well as ecological and atmospheric processes necessitates the prediction of root water uptake (Shukla and Mintz, 1982;Jackson et al., 2000). For this, together with observations, models have become vital tools that are used both in order to gain local process understanding as well as to predict macroscopic root water uptake characteristics.

Water uptake is driven by gradients in water potential, whereby water is pulled up from the soil into the root and up to the leaf (Steudle, 2001;Angeles et al., 2004). Besides soil hydraulic resistance, root tissue resistances determine the actual values of water uptake and water transport (Van Den Honert, 1948): Radial resistance of soil and roots for the flow path across the soil-root-interface and roots axial resistance for the flow path within the root xylem. The ratio between radial and axial resistance is of substantial importance. It shapes the distribution of xylem water potential throughout the root and thus influences root water uptake (Landsberg and Fowkes, 1978). Moreover, Zwieniecki et al. (2003) modelled a trade-off between hydraulically active root length and the corresponding water uptake in unlimited water reservoirs. The term “hydraulically active” corresponds to the portion of the root that considerably contributes to root water uptake. The proposed trade-off hinges upon the ratio of radial and axial root hydraulic resistance: When radial resistance increases, the active root length increases whereas water uptake decreases.

For process studies of root water uptake, models that compute microscopic three-dimensional root water uptake with respect to gradients in water potential and hydraulic resistances have become more and more popular (Clausnitzer and Hopmans, 1994;Tuzet et al., 2003;Doussan et al., 2006;Javaux et al., 2008;Schneider et al., 2010). Most of these models solve water flow equations within soil and root system architecture. They account for the microscopic soil water flow towards individual roots, radial flow into the root xylem and the axial xylem flow

within the root system. The modelling scale of these small-scale approaches comes close to the scale at which root water uptake takes place. Thus, they promise an important contribution to process understanding. Indeed, they capture well observed processes such as redistribution of root water uptake due to local limitations of soil water availability, including moving uptake fronts (Garrigues et al., 2006;Javaux et al., 2008;Schneider et al., 2010) and also hydraulic lift (Dunbabin et al., 2013). This is a major improvement compared to empirical models (Feddes et al., 1978). The inherent redistribution of root water uptake based on explicit calculations of water flow in roots is also reported to be superior to qualitative approaches (Simunek and Hopmans, 2009).

However, parameterization of small-scale models still poses a substantial challenge, since it requires detailed information that are difficult to obtain: (a) on root geometry and even more challenging (b) on distribution of root hydraulic properties. Some progress on point (a) has already been made. Recent improvements in imaging (Oswald et al., 2008;Mooney et al., 2012) and image analysis (Leitner and Schnepf, 2012) have improved information on root system geometry like position, orientation, branching order and root diameter. However, information on root hydraulic properties (point (b)) is still extremely sparse, because the necessary measurements are tedious (Knipfer et al., 2007). Thus, an important input to three-dimensional root water uptake models, that is the exact arrangement of root hydraulic properties within the root system, remains largely unknown.

Modelling results suggest that the lack of knowledge on root hydraulic properties may be a substantial hindrance (Schneider et al., 2010). As stated above, the distribution of water potential and root water uptake along the root system depends dominantly on the ratio between root axial and root radial resistance (Landsberg and Fowkes, 1978;Zwieniecki et al., 2003;Doussan et al., 2003; Levin et al., 2007;Javaux et al., 2008). For what is more, during root maturation individual root hydraulic properties change with time (Steudle, 2000). Older suberized roots with more and mature xylem vessels have lower axial and higher radial resistance compared to younger roots. A root system contains both mature and young roots and observations show that conductivities along the radial and axial pathways vary within several orders of magnitude along root networks (Frensch and Steudle, 1989;Doussan et al., 2006). Hence a root system is a network of elements with contrasting hydraulic properties. Modellers account for this heterogeneity differently. Doussan et al. (2006) distributed hydraulic properties stepwise according to root length in taproots and root age in lateral roots.

Schneider et al. (2010) translated a root developmental stage (obtained with a root generator from Pagés et al. (2004)) into five hydraulic classes with distinct root hydraulic properties. However, as stated earlier, the actual arrangement of hydraulic properties within the root system is most of the time unknown and parameterization is based on scarce quantitative information, and researchers are often left to their intuition. To our knowledge, there exists no systematic investigation on whether and how strongly the spatial arrangement of root hydraulic properties affects model results, although such an analysis would greatly help in making decisions on model parameterization.

Root hydraulic properties do not only shape root water uptake profiles (Landsberg and Fowkes, 1978) and active root length (Zwieniecki et al., 2003), but may also be important for the water relations of a plant, because they contribute to the overall resistance to water uptake of the entire soil-plant-continuum and hence on evolution of xylem potential during the uptake process. Strongly negative xylem water potentials increase the danger of embolism and cavitation of xylem vessels, resulting in a progressive loss of axial hydraulic conductivity (Pockman and Sperry 2000;McDowell et al., 2008). Research suggests that plants operate with little safety margin with regard to danger of embolism across climates (Choat et al., 2012;Choat, 2013;Manzoni et al., 2013). As a consequence, plants probably apply strategies to minimize their vulnerability to cavitation, which includes efficient distribution of resistances within their water uptake apparatus. Therefore, xylem water potential at the root collar recommends itself as a tool for distinguishing efficient from less efficient root parameterizations. On the other hand, if modelled xylem potentials are meaningful they can serve as a valuable model output for example for coupling root water uptake to stomatal control (Tuzet et al., 2003).

This modelling study aims at describing and assessing the combined role of heterogeneity of root hydraulic properties and branching topology on root water uptake dynamics. We also investigate their relation to the spatiotemporal evolution of xylem water potential, the overall efficiency of root water uptake and microscopic and macroscopic water relations including hydraulic lift.

Background

We first use a thought experiment to illustrate that root properties inevitably shape active root length, but more importantly how this root length reflects a minimization of a (time average) overall resistance to root water uptake.

Let us consider an un-branched root strand surrounded by a soil cylinder with uniform soil hydraulic properties and at initially homogenous water potential. Let us further assume that the total amount of root water uptake is constant with time. The xylem potential drops along the root, being most negative near the root collar and less negative at the root tip. At the initial stage water uptake occurs predominantly near the root collar, while the apical parts of the root remain in-active. The inactive parts of the root have also been called "hydraulically isolated" in the past (North and Peterson, 2005;Zwieniecki et al., 2003). Later in time, the spatially confined root water uptake near the collar dries the soil selectively, and soil water potential drops to more negative values there. In order to maintain the rate of root water uptake, the xylem water potential at the root collar has to decrease. Simultaneously the water uptake is redistributed away from the collar into the previously isolated region of the root, where water is still available. Over time, this process activates a successively larger proportion of the root for water uptake. However, this comes at a price since the water has to travel increasing distances within the root xylem and therefore has to overcome increasing root hydraulic resistances. Thus, we may suppose that an optimal root length with minimal time average resistance exists.

In order to be able to calculate total root resistance in a simple manner, we further simplify the problem by considering a single unbranched root strand of length l (m) whose time constant rate of water uptake Q (m³/s) is distributed evenly along its length. We now use the common description of root water uptake as being composed of two pathways: first water flows from the soil across the root cortex into the root xylem (radial pathway) and along the root xylem towards the collar (axial pathway). Thus, the total resistance to root water uptake R_{Total} (s/m²) is composed of the radial and axial resistances R_{Rad} and R_{Ax} (s/m²) acting in series

$$R_{Total} = R_{Rad} + R_{Ax} . \quad (1)$$

Radial resistance to root water uptake can be calculated from a root radial resistivity ρ_{Rad} (s) and scales inversely with the surface area of the root, A_{surf} (m²) (see also Sect. 2). Thus, the radial resistance can always be reduced by prolonging the root:

$$R_{Rad} = R_{Rad}(l) = \frac{\rho_{Rad}}{A_{Surf}} = \frac{\rho_{Rad}}{2 \cdot \pi \cdot r \cdot l} \quad (2)$$

$$\lim_{l \to \infty} R_{Rad}(l) = 0 \quad (3)$$

The root axial resistance on the other hand integrates xylem resistivity ζ_{Ax} (s/m³) over the path towards the collar. Under the above-mentioned assumptions, the average distance of water transport equals $l/2$. The mean axial resistance to root water uptake can therefore be expressed by $\zeta_{Ax} \cdot l/2$, and tends to infinity with greater values of l:

$$R_{Ax} = R_{Ax}(l) = \zeta_{Ax} \cdot l/2 \quad (4)$$

$$\lim_{l \to \infty} R_{Ax}(l) = \infty. \quad (5)$$

Thus, a differential increase in root length at the same time reduces radial resistance and increases axial resistance. This once more suggests the existence of an optimal root length l_{opt} (m) that minimizes the total resistance:

$$\frac{dR_{Total}(l)}{dl} = \frac{dR_{Rad}(l)}{dl} + \frac{dR_{Ax}(l)}{dl} = -\frac{\rho_{Rad}}{l^2} \cdot \frac{1}{2 \cdot \pi \cdot r} + \zeta_{Ax} \overset{!}{=} 0 \quad (6)$$

$$l_{opt}^2 = \frac{1}{2 \cdot \pi \cdot r} \cdot \frac{\rho_{Rad}}{\zeta_{Ax}} \quad (7)$$

Note that this optimal length depends directly on the ratio ρ_{Rad}/ζ_{Ax}, but not on their absolute values, and that $\sqrt{(2 \cdot \pi \cdot r)^{-1} \cdot \rho_{Rad}/\zeta_{Ax}}$ indeed has units of meter.

When root length is shorter than its optimum, an increase in root length decreases overall resistance to root water uptake by increasing the effectively utilizable uptake area. We will refer to this case as “radial limitation”. On the other hand an increase of l beyond its optimal value increases overall resistance, because water has to travel longer distances through the root and in this case the axial resistance term dominates. We will refer to such situations as “axial limitation” in the rest of this paper.

Although we are aware that the above-mentioned example is clearly a simplification, it nevertheless captures a more complex representation of roots in limited water reservoirs. The real uptake process is heterogeneous and transient along the root length, as described above. It is still possible to calculate a pure effective root resistance. Couvreur et al. (2012) nicely accounted for the heterogeneity of the soil water potential by identifying an equivalent soil water potential felt by the root. However, our approach is different as we do not aim to separate the effects of the root from those of the soil. We aimed to understand the combined effects of the root hydraulic architecture and the soil on the collar water potential for different

root hydraulic architectures. We will show later in this paper that a similar optimum corresponding to the effective resistance of the root-soil continuum can be observed when considering an average work per unit water taken up by the root. Please note also, that we put our focus on root water uptake only, combined effects of nutrient uptake or carbon costs (Lynch et al., 2013) are neglected.

The fact that the active root length depends on the ratio of ρ_{Rad}/ζ_{Ax} was confirmed in previous studies (Zwieniecki et al., 2003;Javaux et al., 2008). Typically, ρ_{Rad}/ζ_{Ax} ratios for young roots with low radial and high axial resistance are much lower than those for mature suberized roots with high radial and low axial resistance (Steudle and Peterson, 1998;Doussan et al., 2006;Bramley et al., 2007). Young roots therefore are expected to have much smaller efficient uptake length (in the order of some centimeters) than mature roots. At the same time, observations show that total fine root length in root systems is substantial. In the following we show that this is no contradiction because the active fine root length can be enhanced in branched root systems that are composed of root segments of different ρ_{Rad}/ζ_{Ax} ratios.

Radial and axial limitation may occur in model applications and increase modelled xylem potential and affect processes like hydraulic redistribution. In the following we show that these effects dominate model results in some parameterizations and can be avoided with others.

2 Materials and Methods

In this study we investigate the combined influence of heterogeneity of root hydraulic properties and root system topology (branching structure) on spatiotemporal root water uptake dynamics by the help of a simple and a complex root water uptake model. The simple model serves to describe processes of root water uptake at the single root scale that are hard to disentangle at higher levels of model complexity. Within this section we first describe those two applied models of root water uptake. Second, we explain how the root hydraulic properties were systematically varied within the different root systems. Finally, we introduce two indices that are used to quantify the efficiency of root water uptake in terms of "benefits" and "costs": "Water yield" and "effort". All comparisons of root hydraulic parameterizations in this paper are made using these two criteria.

2.1 Simple root water uptake model for root modules

Root water uptake along single un-branched and branched roots was calculated with a simple root water uptake model (see Figure 1 for the considered root structures). It divides the root into n segments and treats the root as a short network of porous pipes. A number of $n=100$ segments for unbranched roots and $n = 196$ segments for branched root modules showed to be sufficient to prevent us from artifacts (see supplementary). Each root segment is considered to have a cylindrical shape of radius $r^{(i)}$ (m) and length $l^{(i)}$ (m).

Each root segment is provided with a limited soil water reservoir. Water is taken up from closed soil cylinders with radius r_{soil} = 1.2cm surrounding the root segments. The water content within each of those soil cylinders is assumed to be spatially constant, but may be different between soil segments. Soil water flow between the soil cylinders was neglected. All soil cylinders share the same hydraulic properties. The soil water potential $\psi_{Soil}^{(i)}$ (m) within each soil cylinder i is derived from volumetric soil water content $\theta_{Soil}^{(i)}$ (m³/m³) with a van Genuchten parameterization of the soil $\theta_{Soil}^{(i)} = f(\psi_{Soil}^{(i)})$. Parameters are taken from Schneider et al. (2010) and were originally obtained for a sandy soil (see Table 1 for details). Thus, the change in soil water status within the soil cylinders is related entirely to root water uptake or release. Simulations are started with initially uniform water content throughout the entire soil domain. These assumptions are made for reasons of simplicity, and in order to investigate in simple terms the impact of soil water potential distribution on root water uptake distribution for different root hydraulic architectures. The complex root water uptake model explicitly accounts for soil water flow (see Sect. 2.2).

Water transport within the roots follows an axial pathway, while water uptake (flow from the surrounding soil into the root) occurs along the radial pathway only. Water flow along each pathway is governed by gradients in hydraulic potential and resistances, similar to Ohm's law. In either direction, the water flow for a given root segment i is given as:

$$Q_{Rad}^{(i)} = \frac{\psi_x^{(i)} - \psi_{Soil}^{(i)}}{R_{Rad}^{(i)}} \quad (8)$$

$$Q_{Ax,in}^{(i)} = \sum_j \frac{\psi_x^{(j)} - \psi_x^{(i)}}{R_{Ax}^{(j)}} \quad (9)$$

$$Q_{Ax,out}^{(i)} = \frac{\psi_x^{(i)} - \psi_x^{(k)}}{R_{Ax}^{(i)}} \quad (10)$$

where $Q^{(i)}_{Ax,in}$, $Q^{(i)}_{Ax,out}$ and $Q^{(i)}_{Rad}$ (m³/s) are the volumetric rates of water flow along the axial pathway into root segment *i*, out of root segment *i* and along the radial pathway from the soil into root segment *i*, given in; $\psi_x^{(i)}$, $\psi_x^{(j)}$, $\psi_x^{(k)}$ and $\psi_{Soil}^{(i)}$ (m) are the xylem water potentials within the root segment *i*, all subsequently connected root segments *j* and the preceding root segment *k,* as well as the bulk soil water potential within the soil surrounding the root segment *i*; and where $R^{(i)}_{Ax}$ and $R^{(i)}_{Rad}$ (s/m²) are the axial and radial root resistance within segment *i*. The resistances are derived from material properties and scale with geometric dimensions as follows:

$$R_{Ax}^{(i)} = \zeta_{Ax}^{(i)} \cdot l^{(i)} \quad (11)$$

$$R_{Rad}^{(i)} = \frac{\rho_{Rad}^{(i)}}{A_{Surf}^{(i)}} = \frac{\rho_{Rad}^{(i)}}{2 \cdot \pi \cdot r^{(i)} \cdot l^{(i)}} \quad (12)$$

The factors $\zeta_{Ax}^{(i)}$ (s/m³) and $\rho_{Rad}^{(i)}$ (s) are the axial and radial root hydraulic resistivity of root segment *i*. Although the resistances $R^{(i)}_{Ax}$ and $R^{(i)}_{Rad}$ determine water flow along potential gradients in the model, the underlying axial and radial root resistivities $\zeta_{Ax}^{(i)}$ and $\rho_{Rad}^{(i)}$ define root hydraulic properties and can be obtained via measurements. Each root segment obtains root hydraulic resistivities corresponding to two discrete hydraulic classes taken from Schneider et al. (2010) (see Sect. 2.3, and Table 1). Heterogeneity of root hydraulic properties is introduced in roots by associating these different hydraulic classes with different regions of the root system (see below).

As a consequence of mass conservation and the absence of storage capacities within the root, the water mass balance holds for each segment *i*:

$$Q_{Ax,in}^{(i)} + Q_{Rad}^{(i)} = Q_{Ax,out}^{(i)}. \quad (13)$$

By substituting the axial and radial flow rates by equations (8), (9) and (10) for all *n* root segments and by denoting with $Q^{(0)}_{Ax}$ (m³/s) and $\psi_x^{(0)}$ (m) the unknown total outflow and water potential at the root collar, we obtain *n* equations for the *n*+1 unknown xylem water potentials including $\psi_x^{(0)}$. Closure of this system of equations is achieved by fixing a boundary condition at the root collar. In our model, this can either be a prescribed (time

dependent) flux rate $Q^{(0)}{}_{Ax}(t)$ or a constant xylem potential $\psi_x^{(0)}$ at the root collar. The former represents a given transpirational demand of a plant at a given time; the latter is used to simulate a plant under water stress. At the onset of water stress transpiration reduces, as collar potential does not further decrease. All simulations are started with a flux boundary condition until collar potential drops to a critical threshold (here taken as a typical value of the permanent wilting point $\psi_{Crit} = -150m$ (-1.5 MPa) upon which the boundary condition switches to the potential boundary condition $\psi_x^{(0)} = \psi_{Crit} = -150m$, thus mimicking "isohydric plants".

After all soil and xylem water potentials have been calculated, root water uptake rates can be deduced using Eq. (5a). After deriving the water uptake rates at time t (s), soil water status is updated using a steady state approach for a sufficiently short interval of time Δt (s),

$$\theta^{(i)}_{Soil;\,new} = \theta^{(i)}_{Soil;\,old} - \frac{Q^{(i)}_{Rad} \cdot \Delta t}{V^{(i)}_{Soil}} \qquad (14)$$

where $V^{(i)}{}_{Soil}$ (m^3) is the total volume of the soil surrounding the root segment i. The soil water potential decreases correspondingly.

The strongly simplified assumptions in this model allow for investigating the role of branching for root water uptake dynamics, which would be hard to detect at a higher level of complexity. In order to test whether they are reproduced in more realistic conditions, we apply the complex root water uptake model described in the next section.

2.2 Root water uptake model for complete root systems

We modelled root water uptake in complete root systems of a single plant individual with the three-dimensional root water uptake model "aRoot", developed by Schneider et al. (2010). We simulate a pot experiment where a complete root system is embedded in one block of soil. Within this block, soil water flow is gradient driven and numerically calculated with a finite element method solving the three-dimensional Richards equation (Kalbacher et al., 2011; Kolditz et al., 2012). Furthermore, "aRoot" accounts for gradients in soil hydraulic conductivity in the immediate vicinity of individual roots. The model of water flow within the root system is equivalent to the simple model described above. For detailed information about the features of "aRoot", please refer to Schneider et al. (2010). Both the van Genuchten

parameters of the soil and the root hydraulic properties are the same as in the simple model (Tables 1 and 2).

2.3 Systematic variation of root hydraulic properties in roots

Both at the single root and at the single plant scale, the complex process of root maturation is simplified by introducing two discrete root hydraulic classes. These two classes possess both axial and radial resistivities $\zeta_{Ax}^{(i)}$ and $\rho_{Rad}^{(i)}$, as well as different ratios of radial and axial resistivity $\rho_{Rad}^{(i)}/\zeta_{Ax}^{(i)}$. Values are taken from Schneider et al. (2010) and refer to "young" and "mature" roots of a 28 d old sorghum plant. For reasons of simplicity the root radius is set equal to 1 mm for all roots. This simplification has little influence on root resistance, since changes in root radius are small compared to changes in root length (see Eqs. (11) and (12)).

In order to assess the influence of heterogeneity of root hydraulic properties, the distribution of the two hydraulic classes along the roots is varied systematically. For this, we neglect information about root age or geometry, as we do not focus on reproducing a specific plant. However, we assume that mature roots always constitute the basal parts and young roots the apical parts in all roots. This is achieved differently at the single root and at the single plant scale.

Single unbranched and branched root topologies are actually created using total root length, the proportion of young and mature roots, and the number of root tips (branches). Figure 1 illustrates the construction of single root modules for the simple model. In un-branched single roots the mature root is located in the basal, the young root in the apical part of the root strand. We modelled un-branched roots with a total length l_{total} between 1 cm and 800 cm, consisting of between 0 % and 100 % of mature roots. Branched root modules are assumed to have two, three, four or six young root branches (n). All of those branches are distributed evenly along a central mature root strand and have equal lengths, resulting in fishbone-like structures. For branched root modules, l_{total} is varied between 5 cm and 400 cm and the proportion of mature roots varies between 10 % and 90 %. We are aware that un-branched roots of great length are unrealistic. However, this artificial setup allows to assess the efficiency of root water uptake depending on the branching structure.

At the single plant scale, our approach of assigning root hydraulic properties is somewhat different, as root geometry and topology are given a priori. The root system geometry is obtained with the root generator "RootTyp" by Pagés et al. (2004) and the location of the

roots within the soil was kept the same for all simulations (see Fig. 7). The parameters used for "RootTyp" are taken from Schneider et al. (2010) and correspond to a 28 d sorghum plant. The resulting total root length was l_{total} = 9.93 m. In order to investigate the influence of heterogeneous hydraulic properties on spatiotemporal root water uptake and its efficiency, we varied the proportions of young and mature roots in steps of 20 % between 0 % and 100 % on this geometry as follows: First, starting at the outer ends of the root system, all tip segments were classified as young roots. Afterwards, this assignment was iterated with the immediately preceding segments. The assignment is suspended at branching points until all branches associated with this point have been classified entirely (as young roots). If the desired amount of young roots is achieved, the remaining segments are classified as mature roots. This ensures that mature roots are never preceded by young roots and they therefore constitute the basal and apical root part, respectively. Please note that this manipulation of the root properties was not performed in the first place to re-produce a natural plant, but to discover shortcomings in root parameterization.

2.4 Measuring the efficiency of root water uptake

Our study aims at comparing the efficiency of root water uptake in terms of "benefits" and "costs" depending on root topology and the degree of heterogeneity of root hydraulic properties. For that purpose we define two indices: "water yield" and "effort", which we will use to assess the efficiency of the root water uptake process.

Water yield $v(t)$ (m³/m) assesses how much water V_{H_2O} (m³) could be taken up per unit root length under unstressed conditions within a given time:

$$v(t) = \frac{V_{H_2O}(t)}{l_{Total}(t)} = \frac{\int_{\tau=0}^{t} \chi(\tau) \cdot Q(\tau) d\tau}{l_{Total}(t)}, \qquad (15)$$

where $Q(\tau)$ (m³/s) is the transpirational demand at time τ (s) and $\chi(\tau)$ is used to indicate water stress at time τ by zero and one otherwise. Thus, root water uptake under stressed conditions does not contribute to water yield. As stated above, we assume that water stress occurs when xylem water potential at the collar $\psi_x^{(0)}$ (m) drops below $\psi_{Crit}^{(0)} = -150m$ (-1.5 MPa). We normalize by total root length in order to obtain uptake per invested meter root length, and in order to correct for the increased soil water reservoir available to longer roots.

Interpretation of expression (15) simplifies under certain conditions. For all simulations presented in this paper, we will be assuming a time constant transpiration rate $Q(t)=Q$ and a drying scenario. This ensures the existence of a unique point $\tilde{t}$ (s) in time at which water stress occurs. In that case and assuming the absence of storage capacities within the root system, water yield is directly proportional to the cumulative transpirational demand of a plant. If root growth is furthermore neglected (l_{total} = *const.)*, water yield $v(t)$ can be calculated as

$$v(t) = \begin{cases} \dfrac{Q \cdot t}{l_{Total}} & t < \tilde{t} \\ \tilde{v} = \dfrac{Q \cdot \tilde{t}}{l_{Total}} & t \geq \tilde{t} \end{cases} \tag{16}$$

Thus, after water stress occurs water yield remains unaltered and becomes independent of time. Within this paper, we will refer to the above stated conditions and denote "water yield" simply as $\tilde{v}$. The lowercase "*v*" indicates that water yield is a normalized volume of water uptake. However, this does not limit the application of the index to transient conditions.

Effort $w(t)$ (J/m³) is a time dependent quantity that measures the average work $W(t)$ (J) necessary to uptake a unit water $V_{H_2O}(t)$, and is evaluated over a given interval of time. Following thermodynamic principles (see Appendix A), $w(t)$ can be derived from the transpirational demand $Q(\tau)$ and the collar potential $\psi_x^{(0)}(\tau)$ (m). It takes the following form:

$$w(t) = \frac{W(t)}{V_{H_2O}(t)} = \frac{\int_{\tau=0}^{t} Q(\tau) \cdot \psi_x^{(0)}(\tau) d\tau}{\int_{\tau=0}^{t} Q(\tau) d\tau} \tag{17}$$

Effort uses the temporal evolution of xylem water potential at the root collar to estimate the efficiency of root water uptake. In accordance with $\psi_x^{(0)}$ effort has units of a negative hydraulic potential (m or J/m³). Please note that 1 MPa can alternatively be stated as a hydraulic head of 101,97m water column or 10^6 J/m³. The effort $w(t)$ therefore also has units of a specific energy and we refer to the absolute values of w when saying "effort is minimized". According to eq. (17), effort can furthermore be interpreted as a flux-weighted average collar potential. Under the conditions stated above (time constant transpiration rate Q,

a drying scenario with unique occurrence time of water stress ($\widetilde{t}$), eq. (17) simplifies for $t \le \widetilde{t}$ and effort can be described with another interesting meaning:

$$w(t) = \frac{\int_{\tau=0}^{t} Q(\tau) \cdot \psi_x^{(0)}(\tau) d\tau}{\int_{\tau=0}^{t} Q(\tau) d\tau} = \frac{Q \cdot \int_{\tau=0}^{t} \psi_x^{(0)}(\tau) d\tau}{Q \cdot t} = \overline{\psi}_x^0(t) \qquad (18)$$

in which $\overline{\psi}_x^0(t)$ (m) is the time average collar potential between times $\tau = 0$ and $\tau = t$. In contrast to water yield, effort still changes after the onset of water stress. But as this contribution is very small (see App. A) we will approximate with $\widetilde{w} = w(\widetilde{t}) = \overline{\psi}_x^0(\widetilde{t})$ the effort under our specific model conditions. As for water yield, the lowercase "*w*" indicates that effort is a specific (normalized) energy.

Figure 2 illustrates how water yield and effort can be used to compare the efficiency of root water uptake for one branched (green) and one un-branched (red) single root, both sharing the same total length. Under the above-mentioned conditions, they can be deduced from the temporal evolution of xylem water potential at the root collar. As the total root length is the same, water yield, $\widetilde{v}$, is directly proportional to the time at which the plant enters water stress, $\widetilde{t}$. In this case, differences in the respective values of $\widetilde{t}$ are very small. Effort, $\widetilde{w}$, corresponds to the area below the two curves, divided by the respective values of $\widetilde{t}$. The green area is much smaller than the red area which indicates that on average a less negative collar potential and consequently less energy was needed for maintaining root water uptake in the branched root. As all other parameters were equal, this indicates an overall lower resistance to root water uptake experienced by the branched compared to the unbranched root.

In this particular case, the differences in effort are induced by branching (see Sect. 3), and Fig. 2 illustrates that the two efficiency measures actually convey different information. Water yield gives the normalized total amount of water that could be extracted under unstressed conditions. In more general terms, it is simply the water flow over the boundary of the system, and it has been applied before by other researchers to evaluate root parameterizations (Schneider et al., 2010; Javaux et al., 2008). On the other hand effort relates to the time evolution of xylem water potential at the root collar and the work necessary for root water uptake. It depends among others on the total resistance to root water uptake a root

system has to overcome. As far as we are aware of, the index effort is a new way of measuring plant performance, and it carries a physiological meaning.

Please note, that the indices are related, as they both depend the root hydraulic resistance. However, effort carries more information on plant function. Since research suggests that plants operate with little safety margin with regard to danger for embolism across climates, plants should apply strategies to avoid very negative xylem water potentials. As lower effort is tantamount for lower xylem water potentials over the course of time, effort recommends itself as a tool for distinguishing efficient from less efficient parameterizations.

3 Results

Within this section we will present how the distribution of hydraulic properties along roots influences the two model efficiency measures, water yield and effort, as well as root water uptake dynamics in different root topologies. We investigate single un-branched and branched roots as well as entire root systems.

3.1 Effort and water yield in un-branched root strands

Figure 3 shows effort (left) and water yield (right) in un-branched homogenous (top) and heterogeneous (bottom) root strands. All heterogeneous root strands consist of basal mature and apical young roots, the length of both regions was varied independently (see Fig. 1). We can by this means find optimal root lengths in terms of both effort and water yield for different proportions of the mature and young root classes.

For homogenous root strands (top) effort and water yield propose similar optimal root length, but different ones for young and mature roots: Young roots have to be short in order to achieve optimal effort and water yield, whereas mature roots have to be long. Interestingly, the actual values at the respective optima are not much different – it is (almost) as efficient to be a short young root as it is to be a long mature root. Water yield is by far the lesser sensitive of the both measures with regard to changes in root length. Also, mature roots exhibit less pronounced differential changes in effort and water yield than young roots when changing root length.

Results for mixed root strands are shown at the bottom of Fig. 3 with green colour indicating high and red colour indicating low efficiency. Efficiency in heterogeneous strands has only slightly increased compared to those in homogeneous root strands with regard to both effort

and water yield. However, the optimal total root lengths are shorter than expected, in that the optimal mixed root strand is not a composition of an optimal mature root strand and an optimal young root strand. In composed roots some of the water is taken up by the basal mature root part and less water has to be transported through the apical young roots. Therefore drops in xylem potential are smaller, axial limitation is less severe and hydraulically active young root region is extended in composed roots. For this reason, in optimal composed roots the young roots are longer and the mature roots are shorter in comparison with the respective optimal homogenous root strands. This leads to overall shorter composite root strands.

3.2 Effort and water yield in single branched roots

Figure 4 shows the effort in root strands (Fig. 4a) and branched single roots with two, four and six tips respectively (Figs. 4b-d). The root composition is now given by the total root length of the respective root (y-axis) and the proportion of mature roots (x-axis). Colours are the same as in Fig. 3 (bottom right). As above, an optimal branched root is neither a composition of the optimal mature root strand, connected to *n* branches of optimal young root strands nor the optimal mixed root strand, which contains *n* instead of one branches of young roots (the latter one is indicated with a cross in figures 4b-d). While the proportion of mature roots in optimal branched roots decreases disproportionally, the total length of all young roots is almost proportional to the number of tips *n*. The overall total root length is only reduced up to a point. When four or six branches of young roots are contained in the branched root individual young root tips shorten only a little, allowing for the total root length to increase without resulting in increased effort. In this way, branching favours soil exploration, without compromising efficiency. Notably, the effort surface becomes flatter, and hence the domain of nearly efficient hydraulic parameterizations expands with the number of tips.

Similar results are obtained for water yield but results are far less sensitive. Figure 5 shows water yield for root strands (Fig. 5a, equivalent to Fig. 3b, but axis denote for total root length and mature root proportion as in Fig. 4) and branched roots with two, four and six tips (Fig. 5b-d). For all branched roots water yield is nearly constant (little sensitive) within the domain of modelled root compositions and did increase only very little compared to the optimal unbranched strand (see Table 2 for optimal values of water yield and effort).

3.3 Water uptake dynamics and redistribution patterns in single roots

The proportions of root hydraulic properties within a branched or un-branched single root do not only affect the efficiency of root water uptake, but also its location and dynamics. This may even be the case, if the efficiency is similar between parameterizations. Figure 6 depicts root water uptake rates along three exemplarily chosen un-branched root strands of equal length (l_{total} = 0.42 cm), which all share very similar values of water yield and effort. The strands consist of young roots only (red), mature roots only (blue) or are an optimal composition of young and mature roots in terms of effort (green). The latter root strand contains 0.14 m of basal mature roots and 0.28 m of apical young roots. Root water uptake along the root strand is shown from the collar (left) towards the tip (right) for different simulation times, namely t = 0 d (top), t = 4 d (middle) and t = 8 d (bottom).

At the initial stage, the young root strand shows an exponential decrease in root water uptake rate towards the tip, which is hydraulically isolated. In contrast, root water uptake is distributed almost equally along the mature root strand. The initial uptake pattern of the mixed root is a combination: An almost homogeneous uptake rate in the basal mature root part is followed by an increased rate of root water uptake in the young root part, which decays exponentially. After some time (four days in the model), a moving uptake front (MUF) has developed both in the pure young and in the mixed root strand, reaching the root tip after 8 days. Additionally, water uptake rate in the basal mature root part increases in the mixed root strand in the course of time. Root water uptake in the pure mature root strand remains almost unaltered during the entire simulation period. Although the occurrence of moving uptake fronts is accentuated by the neglect of soil water flow within the simple root water uptake model, qualitatively the same results are obtained within the complex “aRoot” model, in which soil water flow is explicitly considered (see Sect. 3.5 and Fig. 7).

3.4 Effort and water yield in entire root systems

In order to quantify what influence the above mentioned small scale processes have at the scale of an individual plant and taking soil water flow into account, we used the detailed three dimensional root water uptake model “aRoot”. We calculated effort and water yield along with spatiotemporal root water uptake for one exemplary root system geometry, which was kept the same for all simulations (see Fig. 7 for geometry). We varied only the proportions of young and mature roots in steps of 20 % between 0 % and 100 % (see Sect. 2.3).

Table 3 shows water yield and effort for these six different hydraulic parameterizations. Both criteria showed lowest efficiency in the homogeneous young root system, followed by the

homogeneous mature root system. Heterogeneous root systems (containing between 20 % and 60 % of mature roots) generally had an increased water yield of up to 25 % and decreased their effort substantially by a factor of 2. Root systems containing more mature roots (80 % and 100 %) showed less increased efficiency. We also repeated our observations with a transient (sinusoidal) transpirational demand and obtained qualitatively the same results (see supplementary).

3.5 Water uptake dynamics and redistribution patterns in entire root systems

As mentioned above, single young and mature roots possess different optimal lengths with respect to both water yield and effort. Efficiency of root water uptake in entire root systems is substantially decreased whenever heterogeneity in root hydraulic properties is neglected. In this section we will investigate to what extent heterogeneity of root hydraulic properties also influences spatiotemporal root water uptake at the single plant scale.

Figure 7 shows the spatial distribution of root water uptake characteristics in a root system containing young roots only (left) and a combination of 40 % mature and 60 % young roots (right). These root systems showed lowest and highest efficiency with regard to water yield and effort respectively.

In the top most part of Fig. 7, time averaged root water uptake rate is depicted along the root system. Regions with negative net uptake (bleeding) are depicted in red, independent of the actual amount of released water. Mean root water uptake rates vary much less in the homogeneous compared to the heterogeneous root system (spanning one order of magnitude compared to three orders of magnitude). This indicates the separation of root function in the heterogeneous root system between uptake roots and transport roots, and is in agreement with the earlier observations in the simple model. Apical young roots have a higher mean uptake rate than inner young roots in both hydraulic parameterizations, which is due to higher root density in the central parts of the root system. The domain of hydraulic lift is noticeably larger in the homogenous young root system compared to all other hydraulic parameterizations. Both, the total length of bleeding roots and the amount of water released decreases with increasing proportion of mature roots, being smallest in the homogeneous mature root system (see also Fig. 9).

The lower part of Fig. 7 shows the magnitude (center) and timing (bottom) of the maximum uptake at each location of the root system. This allows tracking of moving uptake fronts. Within the homogenous root system (left) maximum uptake is almost equal, whereas

differences in the order of two magnitudes exist in the heterogeneous system (right). The timing of the maximum shows how uptake moves evenly away from the collar in the young root system as expected from the simple model (see Fig. 6). The overall maximum uptake rates occur at the outer ends of the root system here. The latter appears counterintuitive, because the uptake at root tips should suffer from hydraulic isolation. The reason is the higher root density at the center, which limits maximum uptake rates there. Axial limitation becomes apparent however in the increased effort of root water uptake in the homogeneous young root system (see Table 3).

In heterogeneous root systems the uptake pattern is more complex than in the homogeneous root system. Maximum uptake rates occur in the young roots, which are located anywhere within the root system. The timing of the maximum uptake shows that uptake fronts move not only outwards but also inwards (see the blue roots in the center of the root system depicted in Fig. 7, bottom right). Inner mature roots are activated late and only if the surrounding soil was not previously dried out by young roots. Together with distant young roots, mature roots contribute the majority to total water uptake after 8 days (see Figs. 7 and 9). This redistribution pattern corresponds to the one observed with the simple model in heterogeneous single roots (Sect. 3.3 and Fig. 6). In the simple model root water uptake was redistributed in two ways: "forward" along young roots towards the root tips by moving uptake fronts; and "backward" away from distal young roots to inner mature roots. In the complex "aRoot" model, which considers root length density and soil water redistribution, a third redistribution pattern is added: Redistribution between different root branches. Root water uptake is distributed away from (inner) branches of young and mature roots as they fall dry in the course of soil drying; and is redistributed towards roots in wetter soils. Altogether, this leads to higher efficiency in heterogeneous root systems compared to homogeneous root systems (see Table 3), which is likely to be due to a more efficient compensation for local water stress.

Regardless of the complex uptake dynamics, heterogeneous root systems show a slightly deeper uptake compared to homogenous ones. Figure 8 shows temporal evolution of the depth z_{50} (m) above which half of the root water uptake occurred. The water uptake of the homogeneous young root system is most shallow, followed by the homogeneous mature root system and all heterogeneous root systems. Over the course of time, z_{50} moves downwards in all hydraulic parameterizations and equilibrates at the onset of water stress, with the homogeneous young root system being most dynamical.

Figure 9 shows the temporal evolution of the mature root's contribution to total root water uptake (Figure 9a) as well as the relative amount of bleeding (Figure 9b) for the different hydraulic parameterizations. Results for homogeneous and heterogeneous root systems are shown in solid and dashed lines, respectively. Within all heterogeneous root systems, water uptake of mature roots is at any time smaller than the mature root proportion, indicating that they function as transport roots. At the beginning of the simulation mature root water uptake decreases: Because of their location in the center of the root system, some mature roots fall dry due to high water uptake from neighbouring young roots. Later, mature roots contribute more water to total uptake, because of the backward redistribution already observed in the simple model (Fig. 6). The maximum contribution of mature roots to total uptake is reached at the onset of water stress when critical xylem water potential is reached.

Hydraulic lift occurred in all root parameterizations. However, the amount of water released by the root system depends on the hydraulic parameterization, with by far highest values modelled for the homogeneous young root system (up to 10 % of total root water uptake rate). The amount of bleeding decreases along with decreasing young root proportion, which is in accordance with the decrease in total root length contributing to bleeding (Fig. 7). It must be stated that bleeding usually occurs at night and may hence not be well captured with the time constant flux boundary condition used here. However, simulations with a sinusoidal day/night cycle of transpiration showed qualitatively the same results (see supplementary).

4 Discussion

We used two models in order to examine to what extent heterogeneity of root hydraulic properties influences root water uptake at two spatial scales. Particularly we introduced two measures to compare the efficiency of root water uptake in terms of "benefits" and "costs": Water yield measures the plants ability to extract soil water before entering water stress; and effort indicates the average energy necessary to take up one unit of water under unstressed conditions. By applying these metrics we were able to derive optimal lengths of single roots with different ratios of radial and axial resistivities. Finally we outlined how the heterogeneous distribution of these two hydraulic properties along entire root systems increases efficiency of root water uptake by allowing more efficient compensation of local water stress and avoiding both axial and radial limitation.

In order to disentangle different processes of root water uptake redistribution acting at the same time, we simplified the model scenarios. First we presuppose soil to have homogenous hydraulic properties and to be homogeneously wetted at the initial stage. Second, soil water redistribution was only considered in the complex "aRoot" model. This rather strong simplification in the simple model facilitates understanding the process of root water uptake redistribution. Qualitatively similar effects were obtained with the complex model which explicitly accounts for soil water flow. Third, the presented results were obtained assuming an idealized drying scenario with a time constant flux boundary condition. We do this mainly to standardize the model scenario and hence facilitate comparison of different hydraulic parameterizations. The general definitions of water yield and effort given in equations (15) and (17) are applicable under arbitrary boundary conditions. In order to validate that our results do not depend on specific assumptions, the same analysis was also performed with a sinusoidal transpiration rate in which results remained qualitatively the same (see supplementary). In particular, the ranking of the six hydraulic parameterizations remained the same with regard to temporal evolution of collar potential, water yield and effort, as well as the amount of simulated hydraulic lift (bleeding).

We combine two approaches from Schneider et al. (2010) and Doussan et al. (2006) to generate heterogeneity of root hydraulic properties in roots: First we use two classes of roots with both distinct radial and axial resistivities (young and mature roots). Second, we systematically change the degree of heterogeneity within the respective root by altering the proportions of these two root classes a priori, and by subsequently neglecting both root growth and maturation during the modelling period. Although roots are reported to alter their hydraulic properties according to parameters like topology, diameter and age (Frensch and Steudle, 1989;Steudle and Peterson, 1998;Doussan et al., 2006), we assume that this will not affect our results at the model time scale. Furthermore, these idealizations allow us to neglect processes (which themselves demand for detailed but mainly unknown information and parameters) and facilitate both the description of root water uptake mechanisms and the detection of axial and radial limitation. Generally, considering for root maturation by incremental changes of hydraulic properties within each class as in Doussan et al. (2006) or the further addition of classes as in Schneider et al. (2010) is possible and would further enhance the complex redistribution patterns described in this paper. The efficiency of a given strategy for root growth also changes with the climate, and in particular with drying and rewetting of the soil by precipitation, which we have not considered in this paper. We expect

that the sensitivity of model results to parameterization will be more pronounced in larger root networks and more realistic situations.

Taken together, we believe our model idealizations serve the purpose of discovering drivers that shape root water uptake patterns which are difficult to discover in more comprehensive simulations. They nevertheless capture the essential features to yield process insight.

The two criteria used to compare efficiency of root water uptake, water yield and effort, relate to different aspects of plant physiology and hydrology. Water yield measures the ability of plants to deplete soil water before transpiration is reduced because of water stress. Due to the importance in soil vegetation interactions, and the fact that it is relatively easy to measure in experiments, transpiration appears in modelling studies of root water uptake (Doussan et al., 2006;Javaux et al., 2008;Schneider et al., 2010). In contrast, temporal evolution of xylem water potential at the root collar is usually not discussed in detail, although it includes information at which average cost the root water uptake was achieved. Large negative xylem potentials may lead to cavitation, i.e. the disconnection of the water column within the xylem conduits and interruptions of water transport (Tyree and Sperry 1989;Pockman and Sperry 2000). As cavitation reduces hydraulic conductivity in root xylem, effort may be related to a plants ability to exploit soil water and to sustain droughts (McDowell et al., 2008). We observe that water yield and effort deliver similar results on the numeric value of optimal root length for a given parameterization, but show different sensitivity, with effort being more sensitive to changes in parameterization than water yield. Thus effort suggests itself as an efficiency criterion which may even be more meaningful to plants than water yield. Thus, together with simulators for root architecture (Pagès et al., 2004;Leitner et al., 2010), and given knowledge of critical xylem pressures effort may be a helpful metric for identifying efficient root hydraulic parameterizations of given species.

We observed that unbranched young root strands possess optimal lengths in the range of some centimetres, whereas optimal length of mature root strands may be in the range of meters. Optimal root length of young root strands already account for the redistribution of root water uptake from dry soils to wetter soils by moving uptake fronts. This compensation of local water stress in young roots extends hydraulically active root length and agrees with other models and observations (Roose and Fowler, 2004;Levin et al., 2007). Nevertheless, young root strands suffer from axial limitation when they are too long. All optimal heterogeneous hydraulic parameterizations were more efficient than the corresponding homogenous ones,

which is intuitive and consistent with observations showing that roots differentiate with maturation (Frensch and Steudle, 1989;Doussan et al., 2006). Thus, maturation on the one hand is meaningful from a hydraulic point of view, as it keeps young roots short. Furthermore, overall root water uptake is much more efficient, when the active length of young roots is increased by branching, since this decreases axial limitation.

For root systems, which divide their functioning root water uptake and transport, active young root length increases. Mature roots with higher axial conductivity act as a transport system for uptake delivered from many individual short young roots with high radial conductivity. In other words, transmitting the collar xylem potential effectively to the young root branches is preferably done by mature transport roots in central parts of the heterogeneous root system. This rather intuitive result needs to be considered when parameterizing models for hydrological applications as it also impacts root water uptake dynamics.

In the more realistic and efficient heterogeneous root systems, spatiotemporal uptake behaviour becomes more complex. As long as the soil is moist, water uptake is achieved through young roots with uptake starting near the branching points, as it was already pointed out by Roose and Fowler (2004) and agrees with experimental results from Zarebanadkouki et al. (2013) on lupines. As the soil around the branching points dries out, water uptake is redistributed to the apical ends of the central young roots by moving uptake fronts. Over the course of time xylem water potential drops to a point where water uptake in mature roots becomes possible and water uptake is redistributed "backward" from young roots to mature roots. At the single plant scale we additionally observe re-distribution of water uptake between different root branches as inner short branches fall dry. Thus, particularly in the heterogeneous root systems, the temporal evolution of water uptake is the result of several interacting re-distribution patterns, which do not only move vertically, but also horizontally, and not only from top to down, but also from bottom up. By this, plants with heterogeneous root hydraulic properties have more possibilities to compensate for local water stress in distinct regions of the root system, which likely leads to increased water yield at decreased effort. Therefore heterogeneity of hydraulic properties should be considered at least up to the single plant scale. Surprisingly, changing the proportion of mature roots between 20 % and 60 % resulted in similar, nearly optimal values of both water yield and effort, suggesting that a precise consideration of heterogeneity may not be necessary.

Heterogeneity of hydraulic properties does also influence other root water uptake characteristics, primarily bleeding. Simulated leakage of water from roots to soil can be associated with hydraulic redistribution of soil water through plant roots as described in Prieto et al. (2012). This redistribution of water into dry soils equilibrates soil water potential and may facilitate less negative xylem water potentials, thus inhibiting cavitation (Domec et al., 2006). Several studies report positive effects of hydraulic redistribution on life span of young roots (Caldwell et al., 1998;Bauerle et al., 2008), the accessibility to nutrients (Ryel et al., 2002) and to water relations in plants and ecosystems (Siqueira et al., 2008;Domec et al., 2010;Brooksbank et al., 2011;Prieto et al., 2012). In contrast, our results show the highest amount of bleeding in the most inefficient root hydraulic parameterization, namely in the homogeneous young root system. This result remained unaltered when a sinusoidal transpirational demand was used instead of a fixed flux boundary condition (see supplementary). This indicates that bleeding in this case did not act to improve the overall water status of the plant. Thus although hydraulic redistribution is frequently observed in the real world (Neumann and Cardon, 2012) its occurrence in models does not necessarily imply efficient parameterization.

5 Conclusion

In this modeling study we show that root hydraulic properties, in particular the ratio of root radial and axial resistivity, determine optimal root length in a drying scenario. We investigate this with two different indices of root water uptake: water yield and effort. Both are suitable to detect efficient lengths of young and mature roots, with effort being more sensitive than water yield. Optimal lengths of un-branched young roots are some centimeters, compared to several meters for mature roots. Efficiency of simulated root water uptake increases, when more young root length can be activated. This necessitates branched systems with heterogeneous root hydraulic properties, which allow for a division of function between water uptake and transport. This finding is supported by simulations in a complex three-dimensional root system, where mature roots contribute disproportionally less to overall root water uptake compared to young roots, suggesting that they act as transport roots. Overall root resistance to root water uptake is reduced substantially by conducting the xylem water potential through mature roots efficiently to a large number of apical young roots, which are sufficiently short to take up water efficiently.

As heterogeneity in root hydraulic properties leads to lower effort, increased water yield and altered root water uptake dynamics, heterogeneity should be addressed in root water uptake models. Overall, parameterization of the root system has a great effect on modeled processes that are of interest for the hydrological and ecological community, such as root water uptake profiles, moving uptake fronts, evolution of collar potential over time, and hydraulic re-distribution. As the exploration of these processes is one of the main purposes for using complex three-dimensional models, we believe that parameterization of root properties warrants more attention. Some root water uptake features are similar within a broad range of efficient heterogeneous parameterizations. Therefore the actual degree of heterogeneity may play a subordinate role for root water uptake simulations, as long as hydraulic heterogeneity is accounted for in a principal way.

Appendix A: The functional form of effort and its dependence on boundary conditions

Any water potential ψ_w (m or 9810 J/m³) describes the specific Gibbs free energy of water (Edlefsen and Anderson, 1948, article 62), comparable to the chemical potential. Differential changes in Gibbs free energy ΔG (J) in a system under consideration over a short period of time Δt (s) are therefore

$$\Delta G = \psi_w \cdot \Delta V_w \tag{19}$$

where ΔV_W (m³) refers to the change of water volume in the system. When the system is closed and the change of energy is caused by a water flow Q_w (m³ /s) over the boundary of the system, the above equation becomes:

$$\Delta G = \psi_w \cdot Q_w \cdot \Delta t \tag{20}$$

Applying these equations to the coupled plant-root system in a closed container, where the only water flow out of the system is by root water uptake, we can therefore state that the change in Gibbs free energy of the system from a starting point t_0 (s) up to a time t (s) under consideration is

$$G(t) = \int_{\tau=t_0}^{t} \psi_C(\tau) \cdot Q(\tau) d\tau \tag{21}$$

where $\psi_C(\tau)$ (m) refers to the water potential at the root collar at time τ (s).

As the change of Gibbs free energy to go from state A to state B of a closed system equals the mechanical work to go from A to B (neglecting the work of expansion, Edlefsen and Anderson, 1948, article 21, 62), $G(t)$ is equivalent to the work required for root water uptake. We can define a normalized measure, $w(t)$ (J/m³), which evaluates average work required per unit of water transpired between t_0 and t:

$$w(t) = \frac{G(t)}{\int_{\tau=t_0}^{t} Q(\tau)d\tau} = \frac{\int_{\tau=t_0}^{t} \psi_C(\tau) \cdot Q(\tau)d\tau}{\int_{\tau=t_0}^{t} Q(\tau)d\tau} \tag{22}$$

This means that under arbitrary boundary conditions effort can be understood as a f**lux weighted average** xylem water potential at the root collar.

Under a drying scenario, root water uptake causes soil water potential to decrease monotonically. Thus, at a unique time $\tilde{t}$ (s) plant water stress occurs. Effort at time $\tilde{t}$ will in this case be denoted by $\tilde{w} = w(\tilde{t})$. Under a time constant transpiration rate $Q(\tau) = Q$, effort $\tilde{w} = w(\tilde{t})$ can be calculated as a **temporal average** xylem water potential at the root collar:

$$\tilde{w} = w(\tilde{t}) = \frac{\int_{\tau=0}^{\tilde{t}} Q(\tau) \cdot \psi_C(\tau)d\tau}{\int_{\tau=0}^{\tilde{t}} Q(\tau)d\tau} = \frac{Q \cdot \int_{\tau=0}^{\tilde{t}} \psi_x^0(\tau)d\tau}{Q \cdot \tilde{t}} = \frac{\int_{\tau=0}^{\tilde{t}} \psi_C(\tau)d\tau}{\tilde{t}} = \overline{\psi_{\tilde{t}}} \tag{23}$$

In contrast to water yield, effort increases under water stress. However, this increase is small as will be shown in the following.

In order to calculate effort at a time $t > \tilde{t}$, we use the general definition of effort and split the integrals in the enumerator and denominator at $\tilde{t}$

$$w(t) = \frac{\int_{\tau=0}^{t} Q(\tau) \cdot \psi_C(\tau)d\tau}{\int_{\tau=0}^{t} Q(\tau)d\tau} = \frac{\int_{\tau=0}^{\tilde{t}} Q(\tau) \cdot \psi_C(\tau)d\tau + \int_{\tau=\tilde{t}}^{t} Q(\tau) \cdot \psi_C(\tau)d\tau}{\int_{\tau=0}^{\tilde{t}} Q(\tau)d\tau + \int_{\tau=\tilde{t}}^{t} Q(\tau)d\tau} \tag{24}$$

We can now insert the flux boundary condition $Q(\tau) = Q$ for times $\tau = 0...\tilde{t}$ and the potential boundary condition $\psi(\tau) = \psi_{crit}$ for times $\tau = \tilde{t}...t$. We obtain

$$w(t) = \frac{\int_{\tau=0}^{\tilde{t}} Q(\tau)\cdot\psi_C(\tau)d\tau + \int_{\tau=\tilde{t}}^{t} Q(\tau)\cdot\psi_C(\tau)d\tau}{\int_{\tau=0}^{\tilde{t}} Q(\tau)d\tau + \int_{\tau=\tilde{t}}^{t} Q(\tau)d\tau} = \frac{Q\cdot\int_{\tau=0}^{\tilde{t}} \psi_C(\tau)d\tau + \psi_{crit}\cdot\int_{\tau=\tilde{t}}^{t} Q(\tau)d\tau}{Q\cdot\tilde{t} + \int_{\tau=\tilde{t}}^{t} Q(\tau)d\tau} \quad (25)$$

If we transform the integrals in the stress periods by replacing $\tau = \tilde{t}...t$ by $\tau = 0...\Delta t$ ($\Delta t = t - \tilde{t}$ is the time since the occurrence of water stress), effort can be expressed as

$$w(t) = w(\tilde{t} + \Delta t) = \frac{Q\cdot\int_{\tau=0}^{\tilde{t}} \psi_C(\tau)d\tau + \psi_{crit}\cdot\int_{\tau=0}^{\Delta t} Q(\tilde{t}+\tau)d\tau}{Q\cdot\tilde{t} + \int_{\tau=0}^{\Delta t} Q(\tilde{t}+\tau)d\tau} \quad (26)$$

By defining $E_U := Q\cdot\int_{\tau=0}^{\tilde{t}}\psi(\tau)d\tau = const.$, $V_U = Q\cdot\tilde{t} = const.$, and $V_s(\Delta t) = \int_{\tau=0}^{\Delta t} Q(\tilde{t}+\tau)d\tau$, effort can be expressed as

$$w(t) = w(\tilde{t} + \Delta t) = \frac{E_U + \psi_{crit}\cdot V_S(\Delta t)}{V_U + V_S(\Delta t)} = w(V_s(\Delta t)) \quad (27)$$

E_U (J) is the (time independent) energy that was necessary to take up water under unstressed conditions, it also is the enumerator of $\tilde{w}$; V_U (m³) is the (time independent) amount of water that was extracted before the onset of water stress, it also is the denominator of $\tilde{w}$; and V_s (m³) is the amount of water that was extracted after the onset of water stress. V_s depends on the duration Δt of water stress.

Using a first order Taylor-approximation of w around $\tilde{t}$ yields

$$w(t) = w(\tilde{t} + \Delta t) = \tilde{w} + (\psi_{crit} - \tilde{w})\cdot\frac{V_s(\Delta t)}{V_u} \quad (28)$$

For $\Delta t = 0$ ($t = \tilde{t}$, the onset of water stress) this approximation gives the correct value $\tilde{w}$ of effort. For $\Delta t > 0$, effort increases linearly with the amount of water V_s extracted under water stress. But as root water uptake rates of stressed plants decrease quickly in a drying soil, effort increases very slowly with time.

Acknowledgements

MB was funded by the Jena School for Microbial Communication (JSMC). AH was supported partly by AquaDiv@Jena, a project funded by the initiative “ProExzellenz” of the German Federal state of Thuringia. We thank Peer Joachim Koch (Max-Planck-Institute for Biogeochemistry, Jena, Germany) and Thomas Kalbacher (Helmholtz Centre for Environmental Research, Leipzig, Germany) for their support with the hard- and software. We thank Axel Kleidon for fruitful comments and discussion on an earlier version of this manuscript.

References

Angeles, G., Bond, B., Boyer, J. S., Brodribb, T., Brooks, J. R., Burns, M. J., Cavender-Bares, J., Clearwater, M., Cochard, H., Comstock, J., Davis, S. D., Domec, J.-C., Donovan, L., Ewers, F., Gartner, B., Hacke, U., Hinckley, T., Holbrook, N. M., Jones, H. G., Kavanagh, K., Law, B., López-Portillo, J., Lovisolo, C., Martin, T., Martínez-Vilalta, J., Mayr, S., Meinzer, F. C., Melcher, P., Mencuccini, M., Mulkey, S., Nardini, A., Neufeld, H. S., Passioura, J., Pockman, W. T., Pratt, R. B., Rambal, S., Richter, H., Sack, L., Salleo, S., Schubert, A., Schulte, P., Sparks, J. P., Sperry, J., Teskey, R., and Tyree, M. T.: The Cohesion-Tension theory, New Phytologist, 163, 451-452, 2004.

Bauerle, T. L., Richards, J. H., Smart, D. R., and Eissenstat, D. M.: Importance of internal hydraulic redistribution for prolonging the lifespan of roots in dry soil, Plant, Cell And Environment, 31, 177-186, 2008.

Blum, A.: Crop responses to drought and the interpretation of adaption, Plant Growth Regulation, 20, 135-148, 1996.

Bramley, H., Turner, D.W., Tyerman, S.D., Turner, N. C.: Water flow in the roots of crop species: The influence of root structure, aquaporin activity, and waterlogging, Advances in Agronomy, 96, 133-196, 2007

Brooksbank, K., White, D. A., Veneklaas, E. J., and Carter, J. L.: Hydraulic redistribution in Eucalyptus kochii subsp borealis with variable access to fresh groundwater, Trees-Structure and function, 25, 735-744, 2011.

Cai, X., Wang, D., and Laurent, L.: Impact of Climate Change on Crop Yield: A Case Study of Rainfed Corn in Central Illinois, Journal of Applied Meteorology and Climatology 48, 1868-1881, 2009.

Caldwell, M. M., Dawson, T. E., and Richards, J. H.: Hydraulic lift: Consequences of water efflux from the roots of plants, Oecologia, 113, 151-161, 1998.

Choat, B., Jansen, S., Brodribb, T.J., Cochard, H., Delzon, S., Bhaskar, R., Bucci, S.J., Feild, T.S., Gleason, S.M., Hacke, U.G., Jacobsen, A.L., Lens, F., Maherali, H., Martinez-Vilalta, J., Mayr, S., Mencuccini, M., Mitchell, P.J., Nardini, A., Pittermann, J., Pratt, R.B., Sperry, J.S., Westoby, M., Wright, I.J., Zanne, A.E.: Global convergence in the vulnerability of forests to drought, Nature, 491, 7426, Pages: 752-755, 2012

Choat, B.: Predicting thresholds of drought-induced mortality in woody plant species, Tree Physiology, 33, 669-671, 2013.

Churkina, G., and Running, S. W.: Contrasting Climatic Controls on the Estimated Productivity of Global Terrestrial Biomes, Ecosystems, 1, 206-215, 1998.

Clausnitzer, V., and Hopmans, J. W.: Simultaneous modelling of transient 3-dimensional root growth and soil water flow, Plant And Soil, 164, 299-314, 1994.

Collins, D. B. G. and Bras, R. L.: Plant rooting strategies in water-limited ecosystems, Water Resour. Res., 43, W06407, doi: 10.1029/2006WR005541, 2007

Couvreur, V., Vanderborght, J., and Javaux, M.: A simple three-dimensional macroscopic root water uptake model based on the hydraulic architecture approach, Hydrol. Earth Syst. Sc., 16, 2957-2971, 2012.

Domec, J.-C., King, J. S., Noormets, A., Treasure, E., Gavazzi, M. J., Sun, G., and McNulty, S. G.: Hydraulic redistribution of soil water by roots affects whole-stand evapotranspiration and net ecosystem carbon exchange, New Phytologist, 187, 171-183, 2010.

Domec, J. C., Scholz, F. G., Bucci, S. J., Meinzer, F. C., Goldstein, G., and Villalobos-Vega, R.: Diurnal and seasonal variation in root xylem embolism in neotropical savanna woody species: impact on stomatal control of plant water status, Plant, Cell And Environment, 29, 26-35, 2006.

Doussan, C., Pierret, A., Garrigues, E., and Pagès, L.: Water uptake by plant roots: II – Modelling of water transfer in the soil root-system with explicit account of flow within the root system – Comparison with experiments, Plant and Soil, 283, 99–117, 2006.

Dunbabin, V. M., Postmam, J. A., Schnepf, A., Pagès, L., Javaux, M., Wu, L., Leitner, D., Chen, Y. L., Rengel, Z., and Diggle, A. J.: Modelling root–soil interactions using three–dimensional models of root growth, architecture and function, Plant Soil, 372, 1–2, 93–124, 2013.

Edlefsen, N. and Anderson, A.: Thermodynamics of soil moisture, Hilgardia, 15(2), 31-298 1943.

El Maayar, M., Price, D. T., and Chen, J. M.: Simulating daily, monthly and annual water balances in a land surface model using alternative root water uptake schemes, Advances in Water Resources, 32, 1444-1459, 2009.

Feddes, R. A., Kowalik, P., Kolinska-Malinka, K., and Zaradny, H.: Simulation of field water uptake by plants using a soil water dependent root extraction function, Journal of Hydrology, 31, 13-26, 1976.

Feddes, R. A., Kowalik, P. J., and Zaradny, H.: Simulation of Field Water Use and Crop Yield, John Wiley & Sons, 188 pp., 1978.

Feddes, R. A., Hoff, H., Bruen, M., Dawson, T. E., Rosnay, P. d., Dirmeyer, P., Jackson, R. B., Kabat, P., Kleidon, A., Lilly, A., and Pitman, A. J.: Modeling Root Water Uptake in Hydrological and Climate Models, Bulletin of the American Meteorological Society, 82, 2797-2809, 2001.

Frensch, J., and Steudle, E.: Axial and Radial Hydraulic Resistance to Roots of Maize (Zea mays L.), Plant Physiology, 91, 719-726, 1989.

Garrigues, E., Doussan, C., and Pierret, A.: Water uptake by plant roots: I – Formation and propagation of a water extraction front in mature root systems as evidenced by 2D light transmission imaging, Plant And Soil, 283, 83–98, 2006.

Hildebrandt, A. and Eltahir, E. A. B.: Ecohydrology of a seasonal cloud forest in Dhofar: 2. Role of clouds, soil type, and rooting depth in tree-grass competition, Water Resour. Res., 43, W11411, doi: 10.1029/2006WR005262, 2007.

Hildebrandt, A., and Eltahir, E. A. B.: Ecohydrology of a seasonal cloud forest in Dhofar: 2. Role of clouds, soil type, and rooting depth in tree-grass competition, Water Resources Research, 43, 2007.

Huszár, T., Mika, J., Lóczy, D., Molnár, K., and Kertész, A.: Climate Change and Soil Moisture: A Case Study, Physics and Chemistry of the Earth, Part A: Solid Earth and Geodesy, 24, 905-912, 1998.

Jackson, R. B., Sperry, J. S., and Dawson, T. E.: Root water uptake and transport: using physiological processes in global predictions, Trends Plant Sci., 5, 482–488, 2000.

Javaux, M., Schröder, T., Vanderborght, J., and Vereecken, H.: Use of a Three-Dimensional Detailed Modeling Approach for Predicting Root Water Uptake, Vadose Zone Journal, 7, 1079-1088, 2008.

Kalbacher, T., Schneider, C., Wang, W., Hildebrandt, A., Attinger, S., and Kolditz, O.: Modeling Soil-Coupled Water - Uptake of Multiple Root Systems with Automatic Time Stepping, Vadose Zone Journal, 10, 727-735, 2011.

Katul, G. G., Oren, R., Manzoni, S., Higgins, C., and Parlange, M. B.: Evapotranspiration: A process driving mass transport and energy exchange in the soil-plant-atmosphere-climate system, Rev. Geophys., 50, RG3002, doi: 10.1029/2011RG000366, 2012.

Kleidon, A., and Heimann, M.: A method of determining rooting depth from a terrestrial biosphere model and its impacts on the global water and carbon cycle, Global Change Biology, 4, 275-286, 1998.

Kleidon, A., and Heimann, M.: Assessing the role of deep rooted vegetation in the climate system with model simulations: mechanism, comparison to observations and implications for Amazonian deforestation, Climate Dynamics, 16, 183-199, 2000.

Knipfer, T., Das, D., and Steudle, E.: During measurements of root hydraulics with pressure probes, the contribution of unstirred layers is minimized in the pressure relaxation mode: comparison with pressure clamp and high-pressure flowmeter, Plant, Cell And Environment, 30, 845-860, 2007.

Kolditz, O., Bauer, S., Bilke, L., Bottcher, N., Delfs, J. O., Fischer, T., Gorke, U. J., Kalbacher, T., Kosakowski, G., McDermott, C. I., Park, C. H., Radu, F., Rink, K., Shao, H., Shao, H. B., Sun, F., Sun, Y. Y., Singh, A. K., Taron, J., Walther, M., Wang, W., Watanabe, N., Wu, Y., Xie, M., Xu, W., and Zehner, B.: OpenGeoSys: an open-source initiative for numerical simulation of thermo-hydro-mechanical/chemical (THM/C) processes in porous media, Environmental Earth Sciences, 67, 589-599, 2012.

Landsberg, J. J., and Fowkes, N. D.: Water Movement Through Plant Roots, Annals of Botany, 42, 493-508, 1978.

Leitner, D., Klepsch, S., Bodner, G., and Schnepf, A.: A dynamic root system growth model based on L-Systems, Plant And Soil, 332, 177-192, 2010.

Leitner, D., and Schnepf, A.: Image analysis of 2-dimensional root system architecture, 19th Conference on Scientific Computing, Vysoké Tatry – Podbanské, Slovakia, 2012, 113-119,

Levin, A., Shaviv, A., and Indelman, P.: Influence of root resistivity on plant water uptake mechanism, part I: numerical solution, Transport in Porous Media, 70, 63-79, 2007.

Lynch, J. P.: Steep, cheap and deep: an ideotype to optimize water and N acquisition by maize root systems, Annals of Botany, 112 (2), 347-357, 2013 [AR1_IC1_RC12].

Manzoni, S., Vico, G., Katul, G., Palmroth, S., Jackson, R. B., and Porporato, A.: Hydraulic limits on maximum plant transpiration and the emergence of the safety-efficiency trade-off, New Phytologist, 198, 169-179, 2013.

McDowell, N., Pockman, W. T., Allen, C. D., Breshears, D. D., Cobb, N., Kolb, T., Plaut, J., Sperry , J. S., West, A., Williams, D. G., and Zepey, E. A.: Mechanisms of plant survival and mortality during drought: why do some plants survive while others succumb to drought?, New Phytologist, 178, 719-739, 2008.

Mooney, S. J., Pridmore, T. P., Helliwell, J., and Bennett, M. J.: Developing X-ray Computed Tomography to non-invasively image 3-D root systems architecture in soil, Plant And Soil, 352, 1-22, 2012.

Neumann, R. B., and Cardon, Z.: The magnitude of hydraulic redistribution by plant roots: a review and synthesis of empirical and modeling studies, New Phytologist, 194, 337-352, 2012.

Nippert, J. B., and Knapp, A. K.: Linking water uptake with rooting patterns in grassland species, Oecologia, 153, 261-272, 2007.

North, G. B. and Peterson, C. A.: Water flow in roots: Structural regulatory features, in: Vascular transport in plants, edited by M. N. Holbrook and M. A. Zwieniecki, Elevier Academic Press, Burlington, MA, USA., p 131-156, 2005.

Oswald, S. E., Menon, M., Carmina, A., Vontobel, P., Lehmann, E., and Schulin, R.: Quantitative Imaging of Infiltration, Root Growth, and Root Water Uptake via Neutron Radiography, Vadose Zone Journal, 7, 1035–1047, 2008.

Pagès, L., Vercambre, G., Drouet, J.-L., Lecompte, F., Collet, C., and Le Bot, J.: Root Typ: a generic model to depict and analyse the root system architecture, Plant And Soil, 258, 103-119, 2004.

Pockman, W. T., and Sperry , J. S.: Vulnerability to xylem cavitation and the distribution of sonoran desert vegetation, American Journal of Botany, 87, 1287-1299, 2000.

Prieto, I., Armas, C., and Pugnaire, F. I.: Water release through plant roots: new insights into its consequences at the plant and ecosystem level, New Phytologist, 193, 830-841, 2012.

Roose, T., and Fowler, A. C.: A model for water uptake by plant roots, Journal of Theoretical Biology, 228, 155-171, 2004.

Ryel, R. J., Caldwell, M. M., Yoder, C. K., Or, D., and Leffler, A. J.: Hydraulic redistribution in a stand of Artemisia tridentata: evaluation of benefits to transpiration assessed with a simulation model, Oecologia, 130, 173-184, 2002.

Schneider, C., Attinger, S., Delfs, J.-O., and Hildebrandt, A.: Implementing small scale processes at the soil-plant interface – the role of root architectures for calculating root water uptake profiles, Hydrology And Earth System Science, 14, 279-289, 2010.

Seneviratne, S. I., Corti, T., Davin, E. L., Hirschi, M., Jaeger, E. B., Lehner, I., Orlowsky, B., and Teuling, A. J.: Investigating soil moisture–climate interactions in a changing climate: A review, Earth-Science Reviews, 99, 125-161, 2010.

Shukla, J., and Mintz, Y.: Influence of Land-Surface Evapotranspiration on the Earth's Climate, Science, 215, 1498-1501, 1982.

Siqueira, M., Katul, G., and Porporato, A.: Onset of water stress, hysteresis in plant conductance, and hydraulic lift: Scaling soil water dynamics from millimeters to meters, Water Resour. Res., 44, W01432, doi:10.1029/2007WR006094, 2008.

Steudle, E., and Peterson, C. A.: How does water get through roots?, Journal of Experimental Botany, 49, 775–788, 1998.

Steudle, E.: Water uptake by plant roots: an integration of views, Plant And Soil, 226, 45-56, 2000.

Steudle, E.: The cohesion-tension mechanism and the acquisition of water by plant roots, Annual review of plant physiologca and plant molecular biology, 52, 847-875, 2001.

Tuzet, A., Perrier, A., and Leuning, R.: A coupled model of stomatal conductance, photosynthesis and transpiration, Plant, Cell And Environment, 26, 1097-1116, 2003.

Tyree, M. T., and Sperry , J. S.: Vulnerability of xylem to cavitation and embolism, Annual review of plant biology, 40, 19-36, 1989.

Van Den Honert, T. H.: Water Transport in plants as a catenary process, Discussions of the Faraday Society, 3, 146-153, 1948.

Ward, D., Wiegand, K., and Getzin, S.: Walter's two-layer hypothesis revisited: back to the roots!, Oecologia, 172, 617-630, 2013.

Zarebanadkouki, M., Kim, Y. X., and Carminati, A.: Where do roots take up water? Neutron radiography of water flow into the roots of transpiring plants growing in soil, New Phytologist, 199, 1034–1044, doi: 10.1111/nph.12330, 2013.

Zwieniecki, M. A., Thompson, M. V., and Holbrook, N. M.: Understanding the Hydraulics of Porous Pipes: Tradeoffs Between Water Uptake and Root Length Utilization, Journal of Plant Growth Regulation, 21, 315-323, 2003.

1 Table 1: Parameters and important features of the simple and the "aRoot" model.

Soil properties	*Simple model*	*"aRoot" model*
Limited water reservoir	Yes	
Gravitation	No	Yes
Redistribution of soil water	No	Yes (3D Richards)
Gradients in soil hydraulic conductivity	No	Yes
Soil porosity	0.46	
Saturated hydraulic conductivity	$1.785 \cdot 10^{-6} \frac{m}{s}$	
n_{VG}	1.534	
α_{VG}	1.44 m^{-1}	
λ_{VG}	-0.215	
Initial saturation	0.9 (r_{soil} = 1.2 cm)	0.4 (V_{Soil} = 60 dm³)

Root properties	*Simple model*	*"aRoot" model*
Heterogeneous root hydraulic properties	Yes	
Critical collar potential	-150 m	
Flux boundary condition $Q(t)$	$5 \cdot 10^{-11} \frac{m^3}{s}$	$3 \cdot 10^{-9} \frac{m^3}{s}$
Total root length l_{total}	0.01 m – 8 m	9.93 m
Branching Order	≤ 1	$>> 1$
Account for root length density	No	Yes
Number of root segments	100 (unbranched) / 192 (branched root)	1412

Root hydraulic properties	*Mature root*	*Young root*
Axial resistivity ζ_{Ax} [s m^{-3}]	8×10^{10}	1×10^{12}
Radial resistivity ρ_{Rad} [s]	5×10^{8}	1×10^{8}

2

Table 2: Optimal compositions of single root modules referring to effort (top) and water yield (bottom). Results are obtained with the simple model for different root topologies.

Structure	l_{total}	l_{mature}	l_{young}	l_{young} per branch	$\widetilde{w}$ [m]
Young root strand	0.20m	-	0.20m / 100%	0.20m	-18.01
Mature root strand	1.60m	1.60m / 100%	-	-	-15.27
Mixed root strand	1.50m	1.20m / 80%	0.30m / 20%	0.30m	-15.05
Branched structure, 2 tips	1.30m	0.65m / 50%	0.65m / 50%	0.325m	-14.36
Branched structure, 3 tips	0.90m	0.09m / 10%	0.81m / 90%	0.27m	-13.45
Branched structure, 4 tips	1.20m	0.12m / 10%	1.08m / 90%	0.27m	-12.84
Branched structure, 6 tips	1.60m	0.16m / 10%	1.44m / 90%	0.24m	-12.26

Structure	l_{total}	l_{mature}	l_{young}	l_{young} per branch	$\widetilde{v}$ [ml/m]
Young root strand	0.15m	-	0.15m / 100%	0.15m	153.07
Mature root strand	1.80m	1.80m / 100%	-	-	153.21
Mixed root strand	1.60m	1.28m / 80%	0.32m / 20%	0.32m	153.21
Branched structure, 2 tips	0.90m	0.27m / 30%	0.63m / 70%	0.315m	153.24
Branched structure, 3 tips	0.90m	0.18m / 20%	0.72m / 80%	0.24m	153.28
Branched structure, 4 tips	1.20m	0.12m / 10%	1.08m / 90%	0.27m	153.30
Branched structure, 6 tips	2.00m	0.20m / 10%	1.80m / 90%	0.30m	153.32

Table 3: Initial collar potential $\psi_x^0(t=0)$, effort $\widetilde{w}$, water yield $\widetilde{v}$ and mean uptake depth z_{50} for one fixed root geometry with a total length of l_{total} = 9.93 m, depending on hydraulic parameterization. Data was obtained with the "aRoot" model for roots containing between 0 % and 100 % of mature roots.

l_{mature}	Ψ_x^0 [m]	$\widetilde{w}$ [m]	$\widetilde{v}$ [ml/m]	z_{50} [cm]
0.00 m (0 %)	-67.03	-105.18	162.13	-6.55
1.99 m (20 %)	-15.72	-44.06	205.43	-6.78
3.97 m (40 %)	-16.75	-42.70	207.45	-6.87
5.96 m (60 %)	-19.09	-46.39	203.42	-6.90
7.94 m (80 %)	-23.55	-54.22	196.37	-6.86
9.93 m (100 %)	-34.72	-77.84	174.22	-6.74

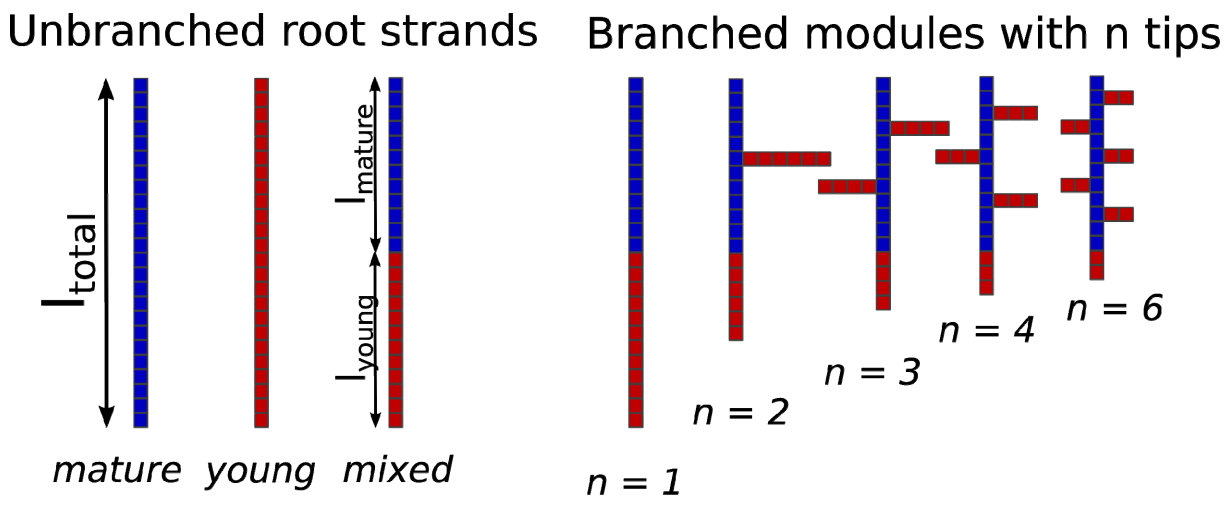

Fig. 1: Schematic representation of the root topologies and parameters that were investigated with the simple root water uptake model. Young (l_{young}) and mature root length (l_{mature}) can be varied independently both in unbranched and branched root structures, resulting in varying total length (l_{total}) and mature root proportion. In all cases mature roots constitute the basal part of the root and are succeeded by apical young roots. Within branched roots, total young root length is evenly divided into n parts, which are attached to the central mature root at equal distances. A mixed root strand can equivalently be regarded as a branched root with n = 1.

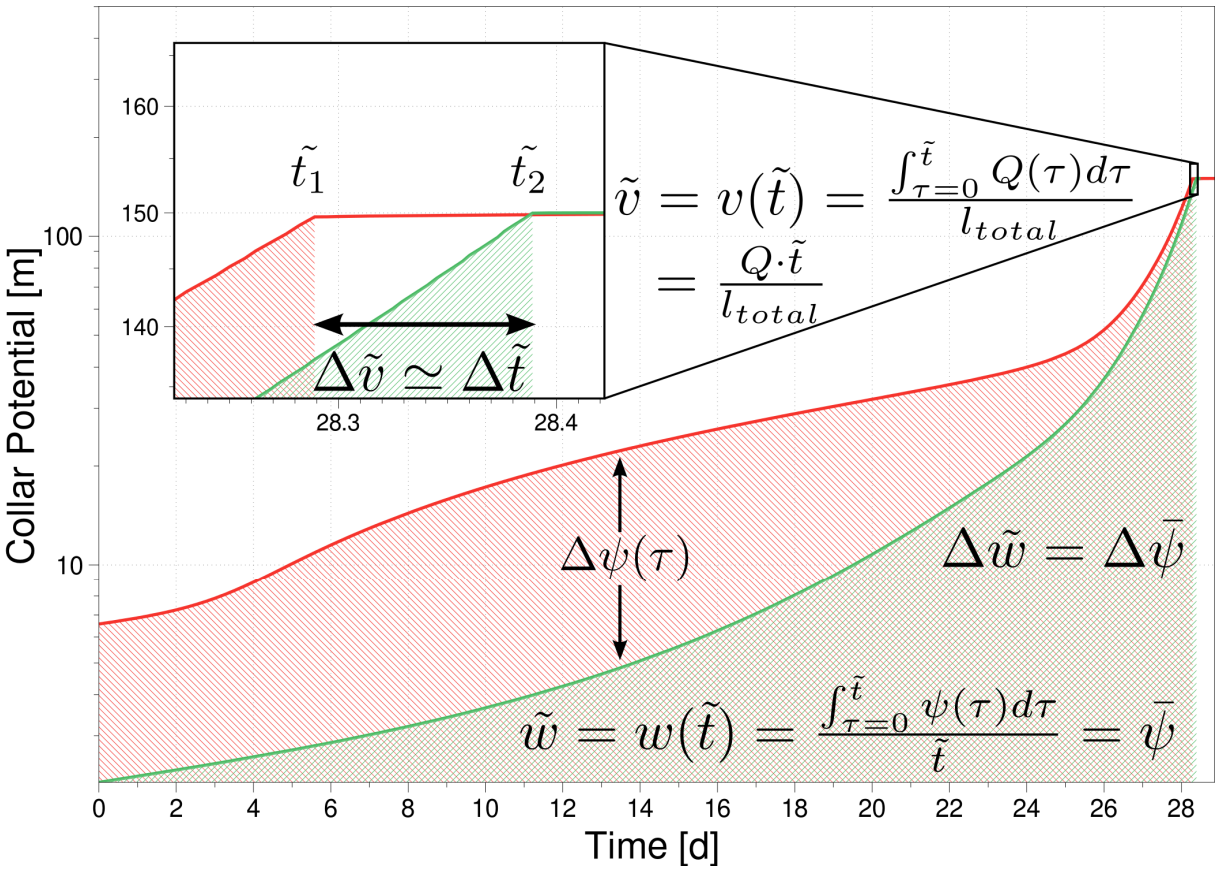

Fig. 2: Evolution of collar xylem water potential over the course of time for two exemplary chosen single roots: an unbranched homogeneous young root strand (red) and a branched structure with six tips (green) of equal length (0.8 m). The two characteristics that are used to assess efficiency of root water uptake, water yield and effort, can be deduced as follows: Water yield is in this case proportional to the occurrence time of water stress, the later collar potential reaches the critical value $\psi_{Crit}^{0} = -150m$ (-1.5MPa) the higher water yield is. Thus, it measures the total amount of water that could be extracted before reaching critical xylem water potential. Effort is a time averaged collar potential and is proportional to the area below the graph. Lower effort corresponds to less negative collar potentials in the course of root water uptake and overall reduced energy necessary for root water uptake. Both measures convey different information: Although water yield is very similar between the two root structures in this case, effort is different.

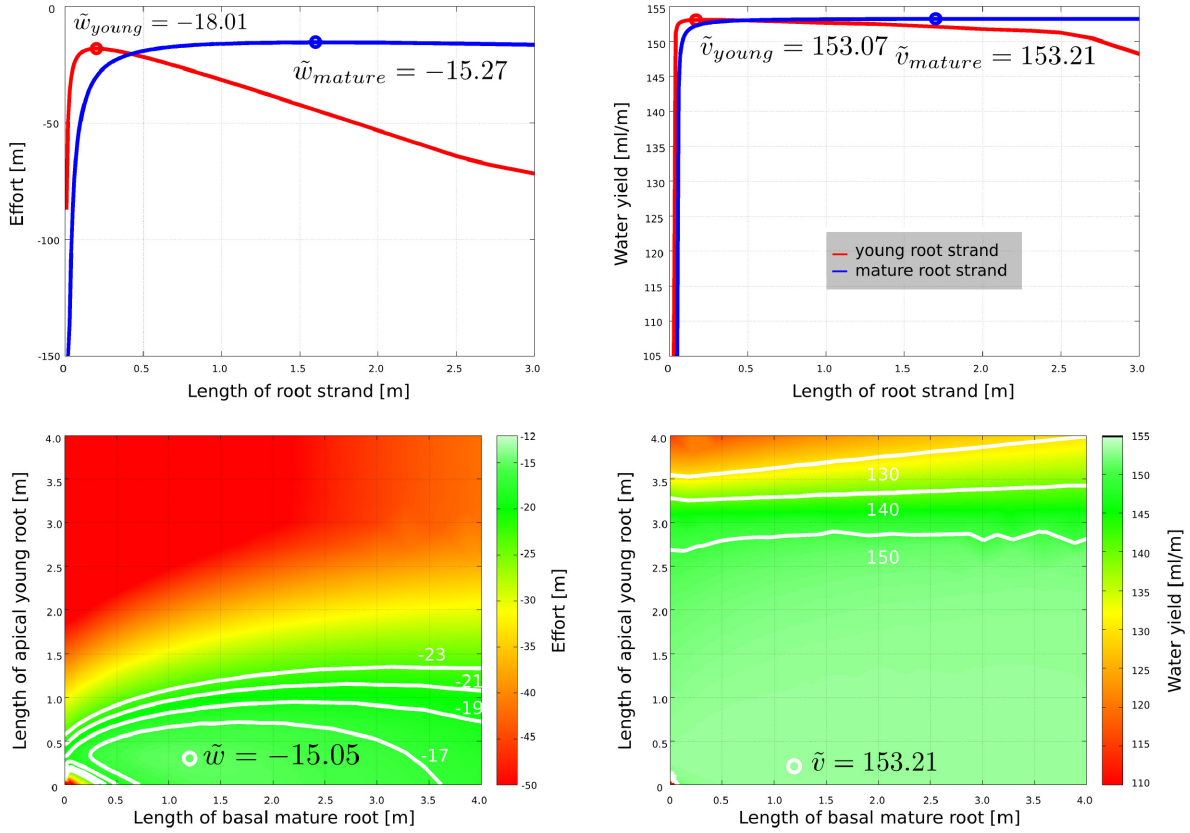

Fig. 3: Effort $\tilde{w}$ (left) and water yield $\tilde{v}$ (right) in un-branched root strands, depending on their composition of young and mature roots. On top effort and water yield are depicted for homogeneous young (red) and mature (blue) root strands over total root length. Below effort and water yield are shown for mixed root strands depending both on mature (x-axis) and young root length (y-axis). Values of effort and water yield are indicated by colors, optimal values are additionally indicated with circles. More negative effort and lower water yield are depicted in red whereas green and light green are indicating higher water yield and less negative effort. Isolines show root compositions that resulted in equal effort and water yield.

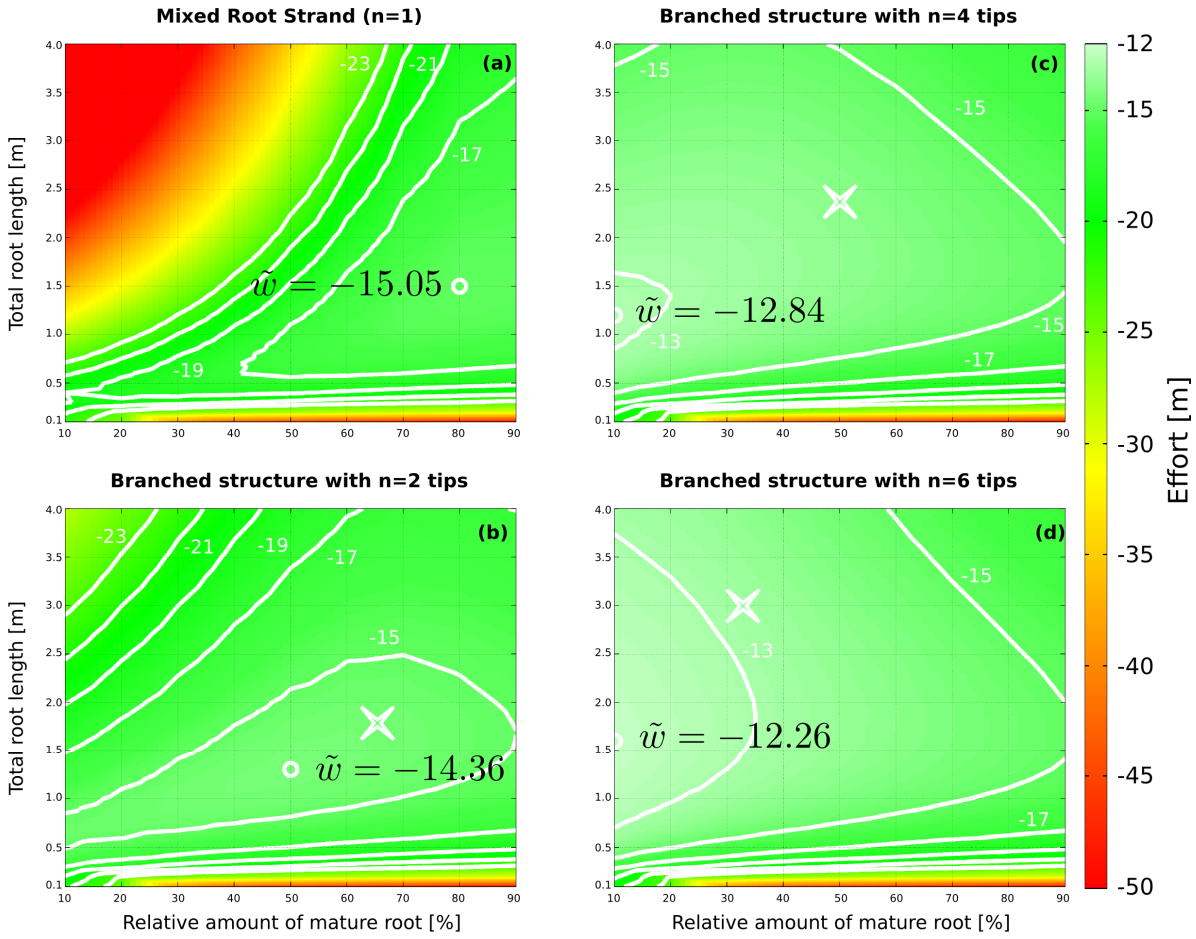

Fig. 4: Effort $\tilde{w}$ depending on topology and composition of single roots. Results are shown for (a) unbranched root strands and single branched roots (fishbone structures) with (b) two, (c) four and (d) six tips. Root composition is given by total root length (y-axis) and the proportion of mature roots (x-axis). Colors are the same as in Figure 3. Data was obtained with the simple model. Optimal values of effort are denoted by white circles, isolines show root compositions that resulted in equal effort. The crosses in figures (b)-(d) indicate effort for a root that is the same as the optimal unbranched mixed strand from (a) except for containing one, three and five more equal young root tips respectively.

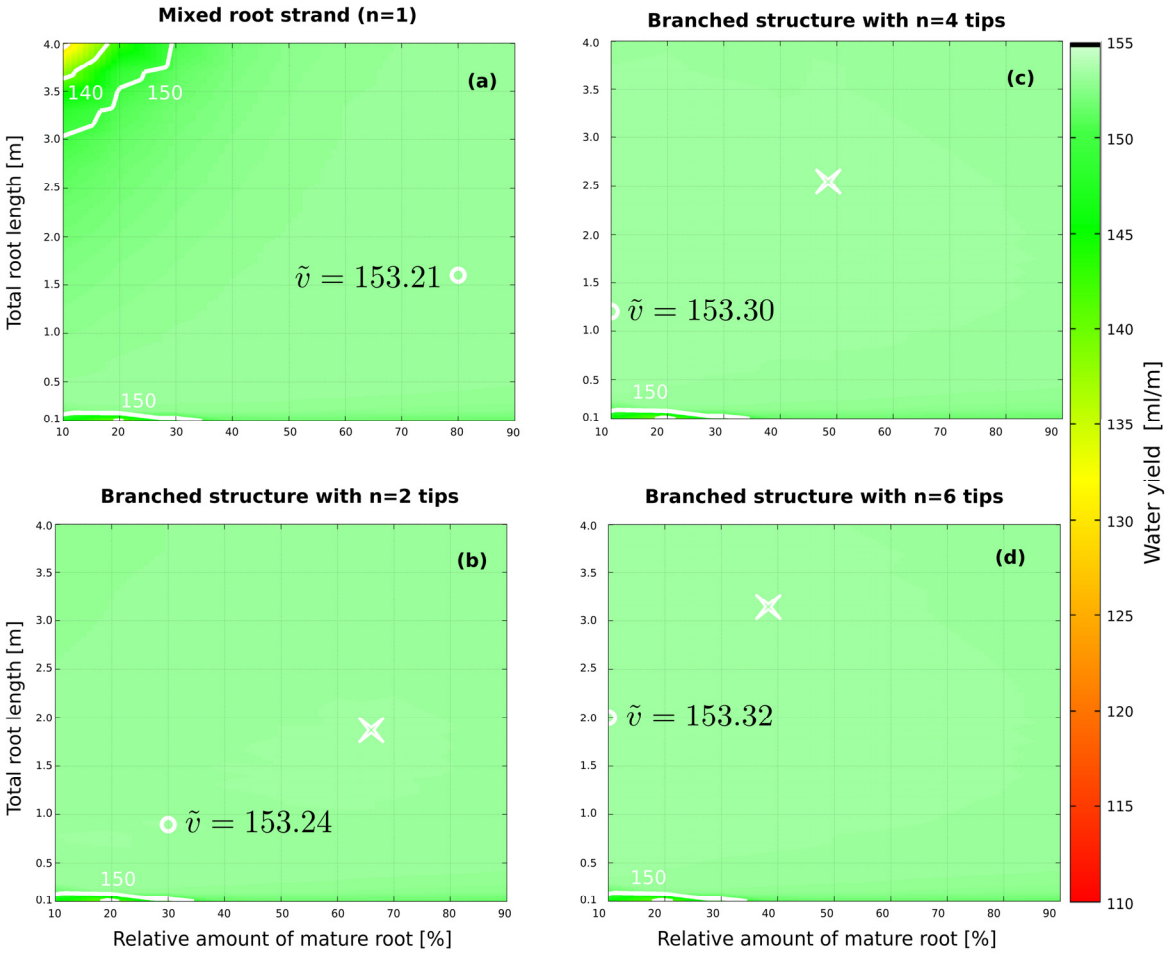

Fig. 5: Water yield $\tilde{v}$ depending on topology and composition of single roots. Results are shown for (a) unbranched root strands and single branched roots (fishbone structures) with (b) two, (c) four and (d) six tips. Root composition is given by total root length (y-axis) and the proportion of mature roots (x-axis). Colors are the same as in Figure 3. Data was obtained with the simple model. Optimal values of water yield are denoted by white circles, isolines show root compositions that resulted in equal water yield. The crosses in figures (b)-(d) indicate water yield for a root that is the same as the optimal unbranched mixed strand from (a) except for containing one, three and five more equal young root tips respectively.

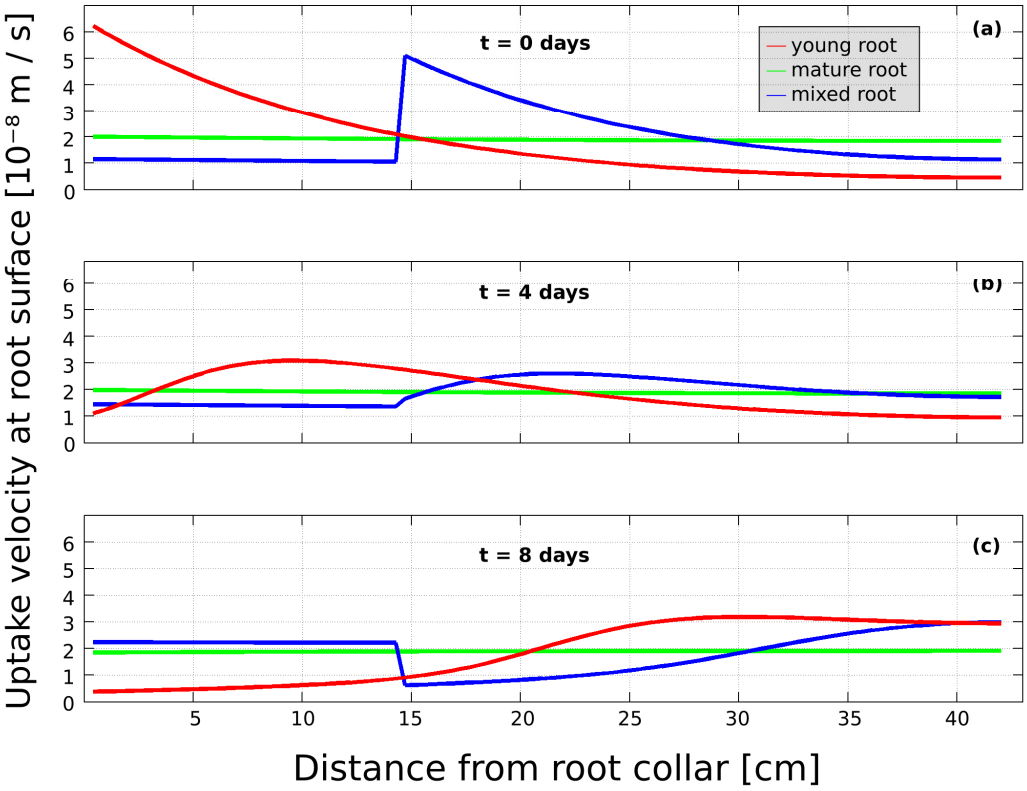

Fig. 6: Velocity of radial inflow (uptake velocity) at the root surface along three root strands with equal length (l_{total} = 0.42 m) but different composition. Values are obtained with the simple model for strands containing young roots only (red), mature roots only (blue) or an optimal mixture with respect to water yield (green; l_{mature} = 0.14 m, l_{young} = 0.28 m). Results are depicted for (a) initial stage, (b) 4 days and (c) 8 days of simulation time.

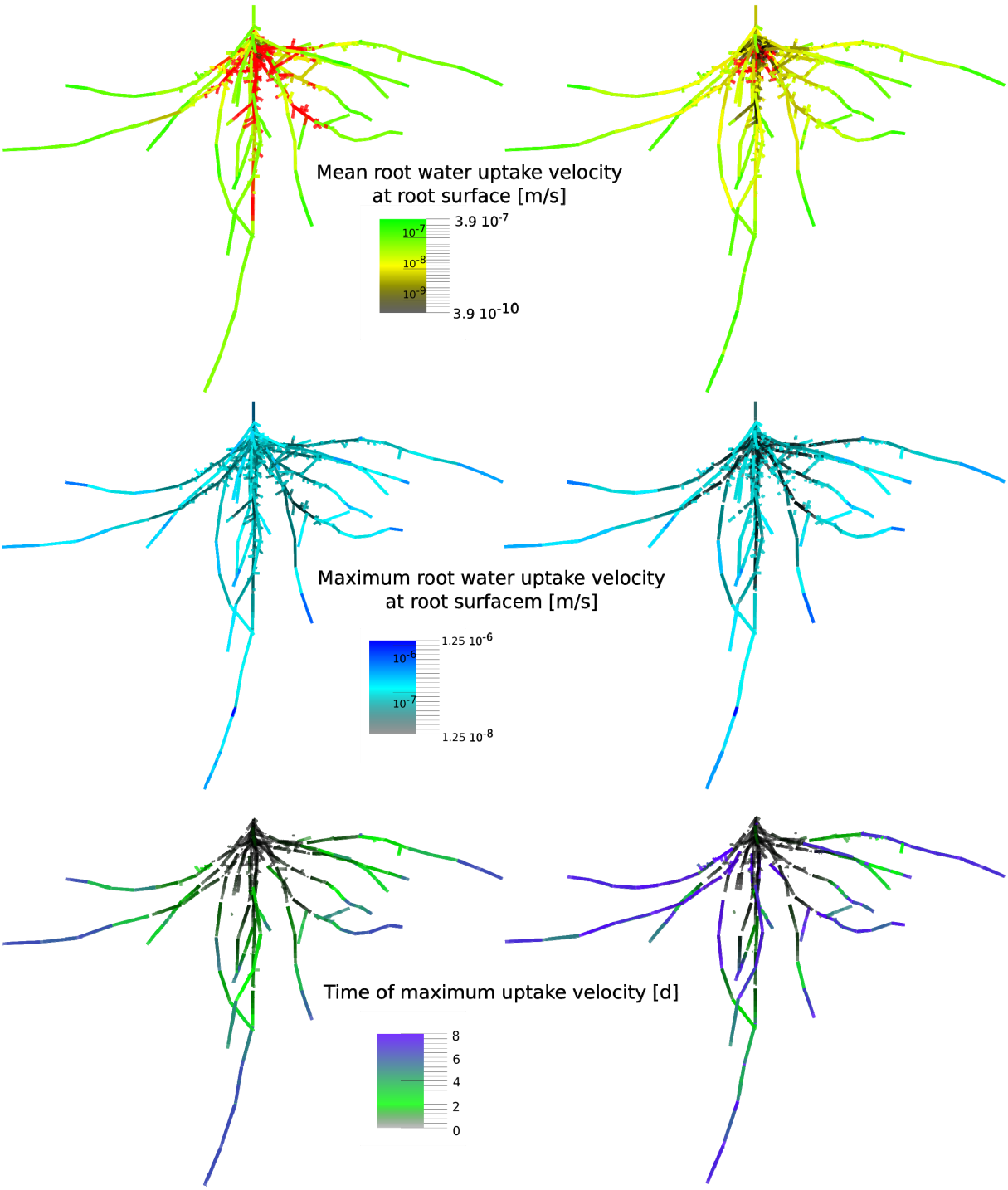

Fig. 7: Root water uptake dynamics in a fixed root geometry under two different hydraulic parameterizations. Data was obtained with the "aRoot" model for one root system containing young roots only (left) and a mixture of 40 % of basal mature and 60 % of apical young roots (right). Time averaged root water uptake rate along the root system is depicted on top. Values cover three orders of magnitude, ranging from black (low values) over yellow to green (high values) on a log scale. Regions with negative net uptake (hydraulic lift or bleeding) are

depicted in red, independent of the actual amount of water released. The lower part of the figure shows the magnitude (center) and timing (bottom) of maximum uptake velocity along the root system. Magnitude of maximum root water uptake ranges over two orders of magnitude and is depicted from black (low values) to blue (high values) on a log scale, whereas timing is given on a linear scale ranging from black (representing initial stages of the simulation) over green to blue (maximum uptake after 8 days).

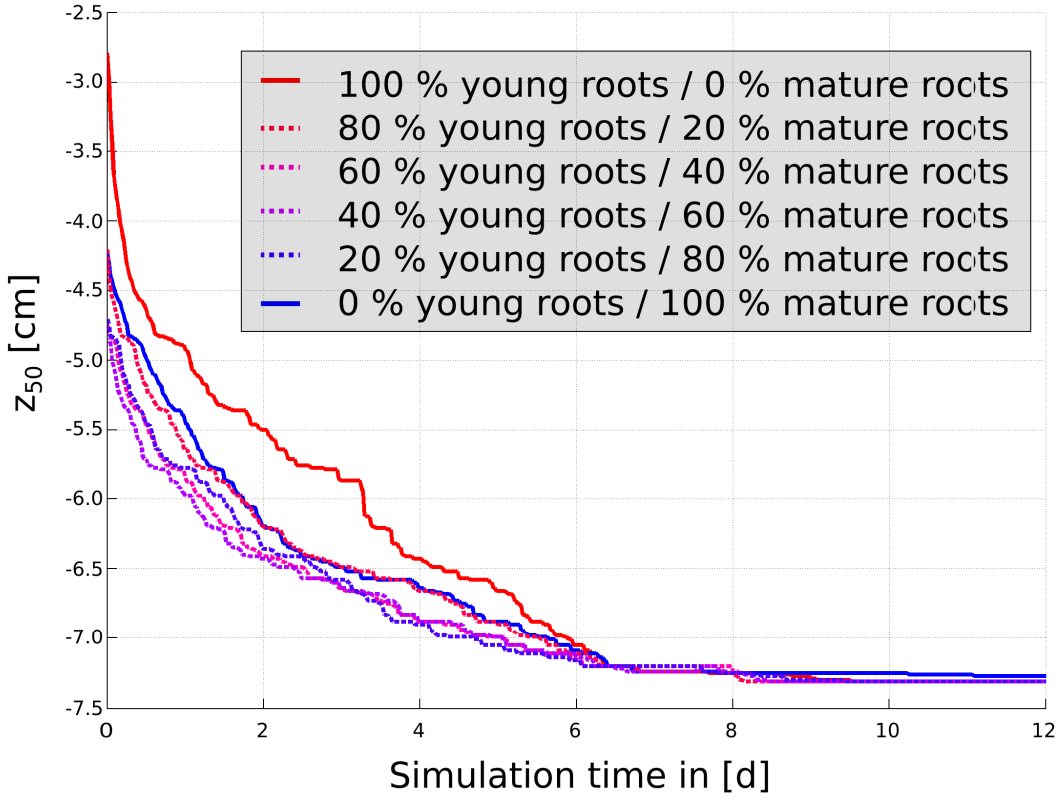

1

2 Fig. 8: Evolution of mean uptake depth z_{50} over time in one fixed root geometry under six
3 different hydraulic parameterizations. Results are obtained with the "aRoot" model for
4 fractions of apical young roots between 0 % and 100 %. Root systems consisting of young or
5 mature roots only are depicted in solid lines; heterogeneous root systems are depicted with
6 dashed lines.

7

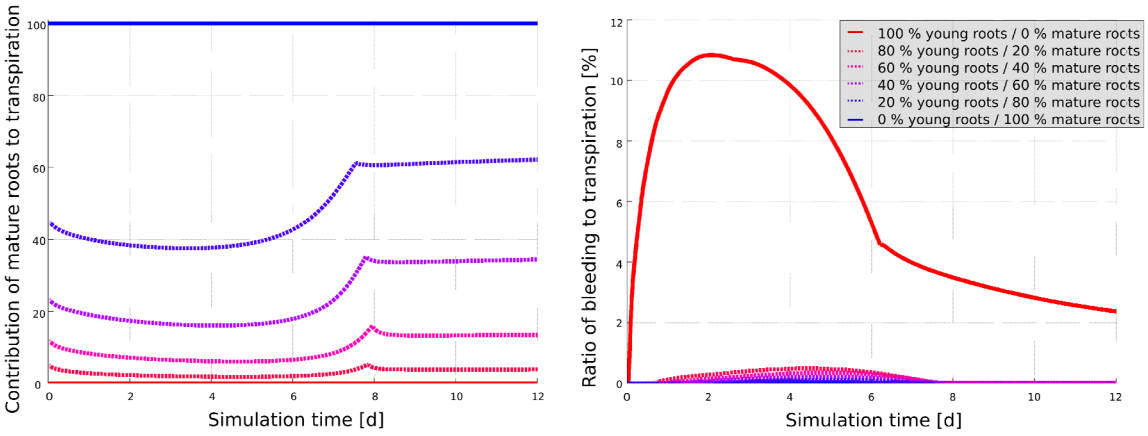

Fig. 9: Evolution of mature root contribution to overall transpiration (left) and the ratio of bleeding (right) over time in one fixed root geometry under six different hydraulic parameterizations. Results are obtained with the "aRoot" model for fractions of apical young roots between 0 % and 100 %. Root systems consisting of young or mature roots only are depicted in solid lines; heterogeneous root systems are depicted with dashed lines.